CHALMERS
UNIVERSITY OF TECHNOLOGY

Tyre Library for Vehicle Energy Model

Master's thesis in Automotive Engineering

POOJA RAMACHANDRA HEGDE

VAMSHI KRISHNA GUNDA

Department of Applied Mechanics
CHALMERS UNIVERSITY OF TECHNOLOGY
Gothenburg, Sweden 2017

Master's thesis 2017:64

Tyre Modelling for On-road and Off-road applications

POOJA RAMACHANDRA HEGDE
VAMSHI KRISHNA GUNDA

CHALMERS
UNIVERSITY OF TECHNOLOGY

Vehicle Dynamics Group
Department of Applied Mechanics
Chalmers University of Technology
SE-412 96 Gothenburg
Gothenburg, Sweden 2017

Tyre Modelling for On-road and Off-road applications
POOJA RAMACHANDRA HEGDE
VAMSHI KRISHNA GUNDA

© POOJA RAMACHANDRA HEGDE,VAMSHI KRISHNA GUNDA, 2017.

Industrial Supervisor: Gunnar Olsson and Brziak Rudolf, at ÅF Industry, Trollhättan
Academic Supervisor: Pär Pettersson, Chalmers Examiner: Prof. Bengt J H Jacobson, Vehicle Dynamics Group, Chalmers

Master's Thesis 2017:64
ISSN 1652-8557
Division of Vehicle Engineering and Autonomous Systems
Department of Applied Mechanics
Chalmers University of Technology
SE-412 96 Gothenburg
Telephone +46 31 772 1000

Cover: artistic illustration of car tyre sinking into soft soil.

Typeset in LaTeX
Printed by Chalmers University of Technology
Gothenburg, Sweden 2017

Abstract

A growing need to minimize fuel consumption motivates research towards energy loss due to tyre components. Performing tyre tests to determine the nature of these losses for every scenario may turn out to be expensive. Magic tyre formula is widely accepted to give comparable results to real world but the model is not motivated with physical principles. An effective tyre model motivated through physical principles that can predict the tyre output characteristics is needed. The key contributors to torque loss in tyres which are rolling resistance and tyre slip losses are studied in this thesis work. The aim of the project was to study the effect of tyre slip and rolling resistance on longitudinal force generation for hard and soft surfaces. The work presented here on is an attempt at arriving at a physical model by improving the basic brush tyre model for hard ground and extending the Bekker-Reece terramechanics theories for deformable ground. The models are built with Matlab scripts and Simulink which gives the user complete flexibility to tune parameters with more test data and customize the models with new additions.

The brush tyre model was improved from the basic model by incorporating different values of friction coefficients for stick region and slip region in the contact patch. Further add-ons for the model with semi-empirical equations are developed by varying friction coefficient with inflation pressure and varying friction coefficient with longitudinal slip to provide the user flexibility to tune parameters in cases where test data is available. The rolling resistance is modelled with an impact loss model that captures variation of rolling resistance force with speed and accounts for a non-zero value of rolling resistance at zero speed. The model used for soft ground is an extension to Bekker's sinkage theory for deformable surfaces and Reece's model that relates sinkage rate of wheel with contact patch pressure. There is also an attempt to introduce an empirical relationship for a special case of tyre and road deforming simultaneously.

The obtained simulation results were compared with available test data for validation. The results show that the extended brush model without the add on is reliable and produces comparable results with test data up to a slip range of 30% where passenger cars operate in normal driving conditions. The model with add-on activated and tuned with test data gives closely matching results for full range of slip. Results for rolling resistance shows that the model captures the nonlinearities for rolling resistance with speed effectively while also having an offset from the origin as desired. Different tyre types are studied here and typical values for the model parameters are tabulated. Simulation results for deformable ground show comparable results with results from research papers conducted for dry sand and soft loam. The model replicates the desirable trends and motivates the obtained results through physical concepts.

Keywords: tyre models, Brush model, Soft ground modelling, Bekker-reece model, rolling resistance, terramechanics, traction, tyres

Acknowledgements

We would like to thank our examiner Prof.Bengt Jacobson and our academic supervisor Lic.Pär Pettersson for their guidance and suggestions throughout this master thesis project. We are grateful for the numerous interesting discussions that have greatly contributed to the completion of this thesis.
We are also very thankful to our supervisors at ÅF consult, Dr.Gunnar Olsson and Civ.Ing.Rudolf Briziak for their valuable inputs and discussions. The weekly meetings were vital in keeping up with the overall project schedule and meet the deadlines.

We want to thank Docent Fredrik Bruzelius from VTI and Lic.Anton Albinsson for providing us with test data for validation of results which was very valuable for the thesis.

Our sincere thanks to Ms. Sreelekha for making the cover art for us.
Lastly, we also want to express our gratitude to our family and friends for their support and continuous encouragement during the stressful weeks of the project.

POOJA RAMACHANDRA HEGDE, VAMSHI KRISHNA GUNDA
Gothenburg, June 2017

List of Symbols

β	shape factor
F_z	normal load [N]
v_x	vehicle velocity [m/s]
R	wheel radius [m]
D	wheel diameter [m]
b	tyre width [m]
H	tread height [m]
T	wheel torque [Nm]
P_i	Tyre inflation pressure [Pa]
T_i	torque loss due to momentum transfer from wheel to ground [Nm]
F_x	longitudinal force at wheel contact [N]
ω	wheel rotation speed [rad]
e	offset distance from wheel centre where vertical reaction force acts at wheel contact [m]
rrc	Rolling resistance coefficient
K_z	Vertical stiffness of the tyre [N/m]
V_x	longitudinal velocity of tyre [m/s]
V_z	vertical velocity of tyre [m/s]
s_x	longitudinal slip
δ	maximum vertical deformation of the tyre [m]
p	momentum of wheel $[kg\frac{m}{s}]$
m_t	mass of wheel [kg]
ε_t	tuning constant for energy loss due to momentum transfer
ε_f	tuning constant for energy loss due to tyre flexing
P_t	power loss due to momentum transfer [W]
P_f	power loss due to tyre flexing [W]
W_f	work done per revolution for flexing of tyre [J]
Fr_{impact}	rolling resistance force due to momentum transfer in tyre
Fr_{flex}	rolling resistance force due to flexing of tyre
Fr	total rolling resistance force
k_1	cohesive modulus of terrain deformation
k_2	frictional modulus of terrain deformation
n	exponent of terrain deformation
z	sinkage depth [m]
c	soil cohesion
ϕ	Friction angle of soil [rad]
γ_s	unit soil weight [kg]
R_0	undeformed tyre radius [m]
c_0	exponent of terrain deformation
c_1	exponent of terrain deformation
m	exponent of terrain deformation
ρ	soil density $[kg/m^3]$
J_x	shear deformation in tyre [m]
k_x	shear deformation modulus [Pa]

Contents

1
Introduction

1.1 Background

The world is moving towards efficient vehicles in terms of energy consumption and is in demand of smart solutions to reduce energy losses. Tyres are one of the important sources for losses in vehicles and the focal point of this work. The main losses in tyres are due to rolling resistance and longitudinal slip, which are considered in this report. To optimize the vehicle efficiency and longitudinal performance, it is essential to have correct model parameterization explaining the physical principles behind the modelling concept.

1.2 Problem motivating the project

It is often difficult to get access to good force-slip characteristics of the tyres when performing energy- and performance simulations in general. In addition, the tyre rolling resistance data is often only available at limited and standard conditions. So, there is a need to develop a tool or tyre model to generate tyre characteristics, based on basic data, physical principles and/or empirical relationships.

1.3 Objective

The objective is to build a model that generates tyre rolling resistance (RR) and longitudinal force and slip data for different tyre and surface types. This model will be used in energy and longitudinal performance simulations with MATLAB and Simulink in different applications under different conditions. Parameters to generate the above data will be presented in a library.

1.4 Deliverables

- Tyre model that generates tyre RR and Longitudinal force and slip data from physical parameters
- A Simulink module that can be implemented in the ÅF energy model
- A library of tyre behavioural response variables based on tyre and road Physical parameters
- A validation of the model using data obtained from running the tyre model in single tyre "virtual test-rig"

1.5 Limitations

- The study is concentrated on only straight line driving conditions. Losses due to lateral slip and aligning moment in the contact patch are not considered
- The study is performed on passenger car tyres and not on truck/motorcycle tyres.
- Only steady-state condition of the tyre strain and stress are considered.

2
Hard Surface

2.1 Tyre Fundamentals

This section aims at looking at a brief description of some of the basic concepts that are relevant to this master thesis project. We consider pneumatic tyres as they are widely used because of superior grip and comfort properties compared to e.g. solid tyres.

2.1.1 Grip on road surface

Tyres are the only components of the vehicle that has direct interaction with the road. They have two fundamental functions, tyres give directional stability and act as drive or brake torque transmission components.

Slippage and Skidding

Tyre slip on the contact patch is produced when the vehicle accelerates, brakes or corners and there is relative motion between contact area and the road.

If we break it down, generating grip involves generating friction forces, F_x in 2.1 which opposes the vehicle's skidding off the road. However, it should be noted that it is the slippage which produces the friction forces for grip, $F_x = f(s_x)$. To summarize, there are two forms of relative motion in the tyre contact patch, micro-motion, explained as slippage, which counteracts the macro-motion, often known as skidding. [16]

2.1.2 Longitudinal Slip

It is defined as ratio of speed difference between tyre and road surface to the reference speed. The reference speed during braking can be vehicle speed v_x, as the objective is to bring the vehicle speed to zero. Similarly it can be the wheel speed $R \cdot \omega$ during acceleration.

Longitudinal slip for positive propulsion, s_x :

$$s_x = \frac{R \cdot \omega - v_x}{|R \cdot \omega|} \tag{2.1}$$

Longitudinal slip for negative propulsion, s_x :

$$s_x = \frac{R \cdot \omega - v_x}{|v_x|} \tag{2.2}$$

2.1.3 Mechanism involved in tyre-road friction

The two shear stresse developed by relative slip between tyre and road surface can be explained on a microscopic level as:

- Molecular Adhesion - At the molecular level where there is attraction between the road surface and the rubber material.
- Hysteresis loss - Loss caused by different paths taken by the rubber material in a stress vs strain diagram for loading and unloading

2.1.4 Influence of road surfaces on the coefficient of friction

The type of road surface plays a major role in tyre interaction with road/soil. Dry asphalt has a high value for friction coefficient as both adhesion and hysteresis losses are high for this surface. Ice on the other hand has very low friction coefficient due to the smooth surface and the adhesion losses are very low. The values change with the surface material and temperature. It becomes even more complex if there are multiple surfaces or mixture of different surfaces.

2.1.5 Rolling Resistance

Rolling resistance (RR) is one of the major contributors for energy loss in tyres. It becomes crucial to study RR for different tyres to reduce fuel consumption. Modern tyres have less RR compared to old tyres. It is important to see how RR varies with different tyre design parameters in order to optimize and select appropriate tyres.

We get the better understanding of the rolling resistance effect on the whole vehicle by looking at the equation of motion as a whole with gradient and aerodynamic resistances included

$$m\dot{v} = \frac{T}{R_l} - F_{roll,driven} - F_{roll,undriven} - F_{grade} - F_{air} \tag{2.3}$$

Where T is the wheel torque coming from the propulsion system or brake system. Rolling resistance force is defined as a resistance to motion of the wheel. Consider the rolling wheel with a normal load of F_z and a loaded radius of R_l shown in figure 2.1.

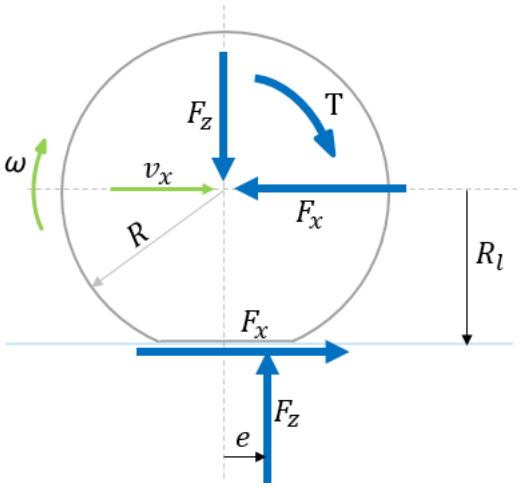

Figure 2.1: Driven wheel with rolling resistance

As the wheel moves forward, the pressure distribution at the contact patch shifts from the line of symmetry of the wheel. This results in an offset e from the centre where the reaction force acts. Taking moments about the wheel centre, we have

$$F_x = \frac{T}{R_l} - F_z \cdot \frac{e}{R_l} \tag{2.4}$$

The quantity $\frac{e}{R_l}$ in the above equation is termed as co-efficient of rolling resistance (rrc). Hence the expression for rolling resistance coefficient becomes

$$rrc = \frac{\frac{T}{R_l} - F_x}{F_z} \tag{2.5}$$

2.2 Simple Brush Model

The brush model is often used to explain how tyres develop traction forces in the road-tyre contact patch. This model describes the physics behind the tyre behaviour at local level, for each contact point in the contact patch.

The tyre contact patch is separated into adhesion and sliding region, shown in fig 2.2. In the adhesive region, the bristles are adhered to the road surface and the force generations is due to static friction. In the sliding region, the bristles slide on the road surface due to the influence of sliding friction. Hence, the resulting force generation in sliding region is independent of the bristle deformation.

This report aims to improve the simple brush model to estimate the traction forces in the tyres as close to real behaviour, which can be compared to magic tyre formula as depicted in the below figure.

2.3 Improved Brush Model

Improved brush model, uses the following assumptions that are different in ways (points 2-4) from simple brush model and brings closer to measured tyre characteristics:

- Sliding and shear stress only in longitudinal direction
- Parabolic pressure distribution over the contact patch, where as simple brush model typically assumes uniform pressure distribution
- Contact length is calculated as a function of vertical force, where as in simple brush model it is known as constant value
- Difference between static and dynamic coefficient of friction, where as in simple brush model there is no difference
- Steady state operating conditions like temperature.

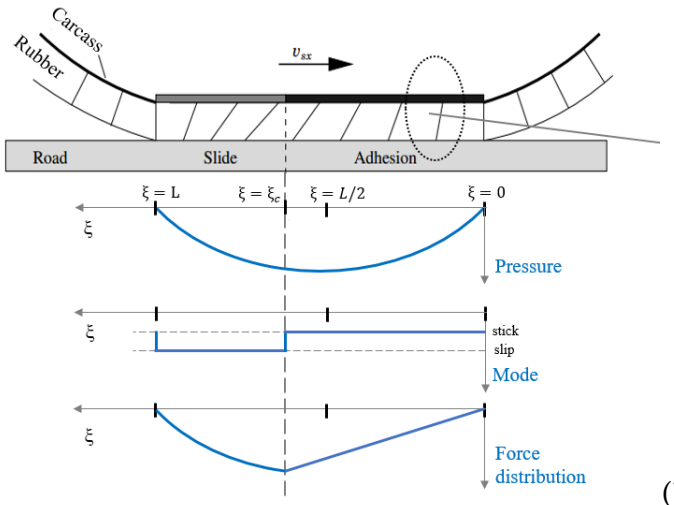

(a)

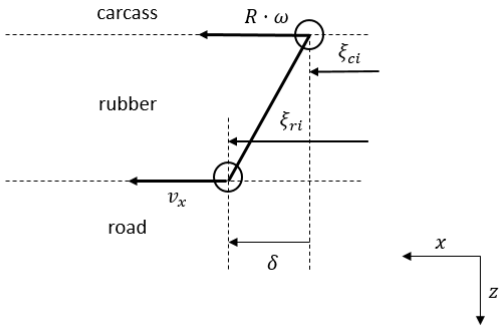

(b)

Figure 2.2: (a): Physical model of tyre brush model for longitudinal slip, (b): velocity of upper and lower points in a cross section of brush element [5]

Lets consider a brush element i, which comes in contact with road surface at position $\xi = 0$ and time $t = 0$ then sticks to the road till breakaway point at $\xi = \xi_c$ and time $t = t'$ and slips thereafter and finally leaves the road surface at $\xi = L$. The position of an element i can be defined by its upper point (ξ_{ci}, attached to the carcass) or its lower point(ξ_{ri}, contact point on the road), see fig 2.2(b).

In adhesive region, the brush elements stick to the ground and their positions are defined by

$$\begin{aligned} \xi_{ci} &= \int_0^{t'} R\omega \; dt \\ \xi_{ri} &= \int_0^{t'} v_x \; dt \end{aligned} \tag{2.6}$$

The longitudinal deformation of an element in the adhesion region is:

$$\delta_i = \xi_{ci} - \xi_{ri} = \int_0^{t'} (R\omega - v_x)\ dt = \int_0^{t'} v_{sx}\ dt \tag{2.7}$$

There comes the discussion whether to use carcass plane ξ_c or road plane ξ_r as longitudinal reference plane ξ for further equations. Rubber bristles are attached firmly to the carcass and equally spaced there i.e, the bristles spacing $d\xi_c$ is constant at carcass plane and $d\xi_r$ at road plane is not constant. So, we use carcass plane as reference for further equations.

Assuming constant velocities, (2.7) with (2.6) gives:

$$\delta = v_{sx}\frac{\xi_{ci}}{R\omega} = s_x \cdot \xi \tag{2.8}$$

where $v_{sx}/R\omega$ is longitudinal slip, s_x as per (2.2)

The rubber elements develop shear stress governed by Hooke's law:

$$\tau = G \cdot \gamma \tag{2.9}$$

where τ is shear stress, G is shear modulus and γ is shear deformation angle

$$\gamma = \frac{\delta}{H} \tag{2.10}$$

where H is tread height.

Combining these equations:

$$\tau = G \cdot \frac{s_x \cdot \xi}{H} = C_x = \frac{G \cdot W \cdot L^2}{2 \cdot H} = \frac{2 \cdot C_x \cdot s_x \cdot \xi}{W \cdot L^2} \tag{2.11}$$

where C_x is the longitudinal slip stiffness, L is tyre contact patch length and W tyre contact patch width, $W = (0, b]$ where b is tyre geometric width.

The friction is assumed to be constant but has different value depending on which region the bristles are operating on the road. Introducing two different friction coefficients, μ_{stick} for stick friction and μ_{slip} for sliding friction, gives more realistic approach for brush model with a peak in non linear tyre characteristic curves, see fig 2.4

Also the symmetric parabolic pressure distribution $p(\xi)$ is defined by:

$$p(\xi) = \frac{6 \cdot F_z}{W \cdot L^2} \cdot \xi \cdot (1 - \frac{\xi}{L}) \tag{2.12}$$

where F_z is normal load on the tyre

The break-away point $\xi = \xi_c$ is defined where the friction limit is reached, $\tau = \mu_{stick} \cdot p(\xi)$

$$\begin{aligned} \tau(\xi_c) &= \frac{2 \cdot C_x \cdot s_x \cdot \xi_c}{W \cdot L^2} = \mu_{stick} \cdot p(\xi_c) \\ \Rightarrow \xi_c &= (1 - \frac{C_x \cdot s_x}{3 \cdot F_z \cdot \mu_{stick}}) \cdot L \end{aligned} \tag{2.13}$$

The expression for longitudinal force becomes

$$F_x = \underbrace{W \cdot \int_0^{\xi_c} \frac{2 \cdot C_x}{W \cdot L^2} \cdot s_x \cdot \xi \; d\xi}_{\text{stick}} + \underbrace{W \cdot \int_{\xi_c}^{L} \mu_{slip} \cdot p(\xi) \; d\xi}_{\text{slip}} \tag{2.14}$$

Simplifying further yields the final expression as:

$$F_x \cdot sgn(s_x) = \begin{cases} \mu_{slip} \cdot F_z & \text{if } \; \omega \cdot v_x < 0 \\ C_x \cdot |s_x| - (2 - \frac{\mu_{slip}}{\mu_{stick}}) \cdot \frac{(C_x \cdot |s_x|)^2}{3 \cdot \mu_{stick} \cdot F_z} + (3 - 2\frac{\mu_{slip}}{\mu_{stick}}) \cdot \frac{(C_x \cdot |s_x|)^3}{27 \cdot (\mu_{stick} \cdot F_z)^2} & \text{else if } \; |s_x| < \frac{3\mu_{stick} \cdot F_z}{C_x} \\ \mu_{slip} \cdot F_z & \text{else} \end{cases} \tag{2.15}$$

2.3.1 Contact patch length

The tyre contact area with road surface is assumed to be approximately rectangular. The width of the contact patch area is assumed to be width of the tyre, but in reality it can be less than this value and at maximum it reaches the width of the tyre. This variation has less effect on the simulation results and assumed to be operating at maximum value all the time.

Contact patch length is derived based on the vertical deformation of the tyre in the contact patch. Deformation is dependent on the vertical stiffness of the tyre.
Using an inextensible ring model, a simple vertical stiffness relationship was derived where the vertical stiffness of the tire, K_z is a proportionality constant between tyre load F and deflection z [4]. In other words it is the secant stiffness expressed as F_z/z. The model inputs parameters are the inflation pressure, the diameter of the tyre and the rolling tread width. These inputs are related to general tyre design parameters and not to the detailed tyre architecture.

$$K_z = 2.74 \cdot P_i \cdot \sqrt{b \cdot (2 \cdot R)} + 33800 \tag{2.16}$$

The units are K_z N/m, P_i in Pa , b in m, and R in m. The constant at the end of the formula, 33800 N/m , represents the zero inflation pressure residual stiffness of the tyre, usually called the structural stiffness.

The equation (2.16) can estimate the vertical stiffness K_z for a wide range of pneumatic tyres and shown to be valid for a variety of belted radial tyre sizes, from passenger car to heavy truck, with no change in the constants. The modelled stiffness values lie within 10% of the measured value.

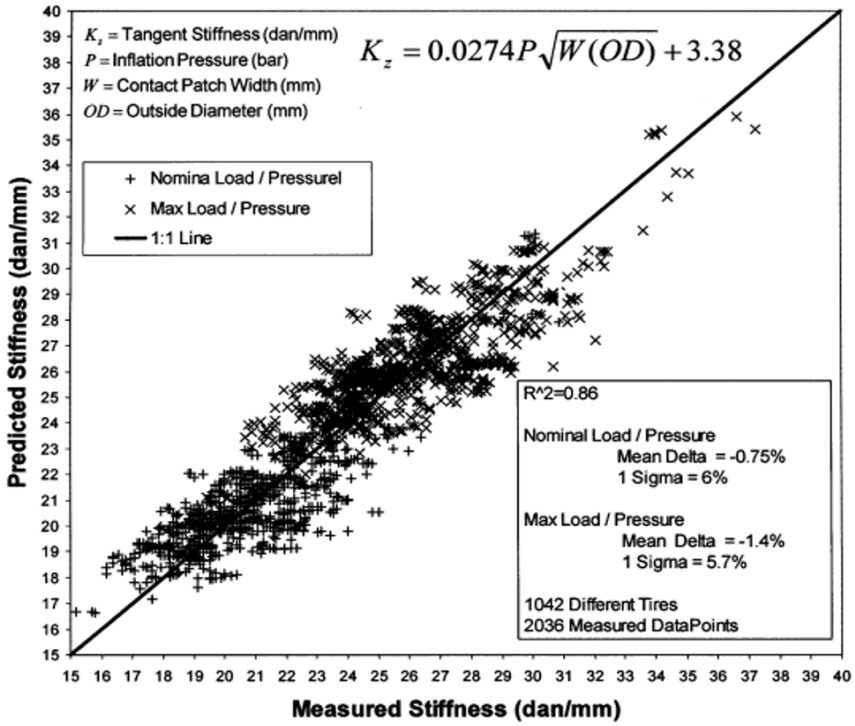

Figure 2.3: The stiffness formula applied to a large body of passenger car data. Predicted vs. measured vertical stiffness [4]

2.3.2 Calibration of the Model

This section analyses the effect of different stick and slip friction coefficients introduced in (2.15)

The calibration factor β is introduced to tune the shape of the force/slip curve for given braking stiffness and peak brake force.

$$\beta = \frac{\mu_{stick}}{\mu_{slip}}, \qquad \geq 1 \tag{2.17}$$

This approach realizes that the peak brake force is lowered as the factor β is increased. In order to attain the same peak brake force value, the static friction is adjusted and a derivation is shown.
By differentiating (2.15) with s_x, the slip where the force has its maximum is given by:

$$\frac{\partial F_x}{\partial s_x} = 0, \Rightarrow s_{x,peak} = \frac{3 \cdot \mu_{stick} \cdot F_z}{C_x \cdot (3 - 2\frac{\mu_{slip}}{\mu_{stick}})}; \quad for \;\; |s_x| < \frac{3 \cdot \mu_{stick} \cdot F_z}{C_x} \tag{2.18}$$

and the peak longitudinal force is

$$F_{x,peak} = \frac{(4\mu_{stick} - 3\mu_{slip})\mu_{stick}^2}{(3\mu_{stick} - 2\mu_{slip})^2} F_z \tag{2.19}$$

In order to adjust the same peak force for changing β, the static friction can be expressed from the (2.19) by $\mu_{static} = \frac{F_{x,peak}(3\beta-2)^2}{\beta F_z(4\beta-3)}$

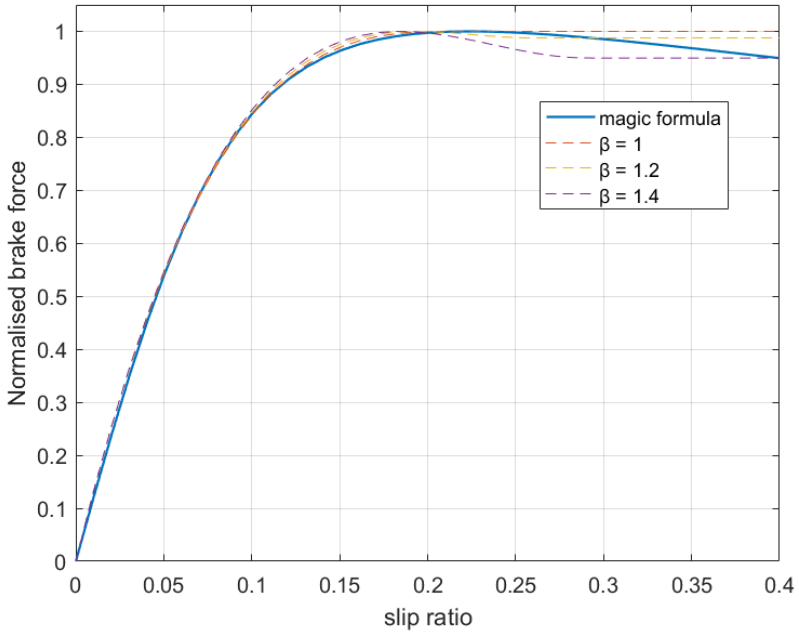

Figure 2.4: Normalized force-slip curve derived by the brush model with different friction values for adhesive and sliding areas. Solid line is the Magic Formula estimated from real data and Dashed curve has $\beta = 1$, 1.2 and 1.4

In fig 2.4 the force-slip curve is plotted for different values of β and compared against Magic tyre Formula.

The calibration factor β depends majorly on the surface and is fairly assumed constant for a given surface during simulations. Based on the simulation results in comparison to the measured data, the following range of typical values is suggested.

Table 2.1: Typical Calibration factor β values suggested for different surfaces

Road type	β **values**
Asphalt	1.2 - 1.8
Snow	1 - 1.2
Ice	1

Further in this report, the same approach of velocity dependent friction has been used extensively to generate the results.

2.4 Add-ons to the Brush Model

To increase the flexibility of the brush tyre model, the simple physical approach is to introduce a sliding-velocity dependent friction coefficient. This approach gives good results at low slips and saturates to a constant value at high slip, see 2.7(a).

In addition to the above approach, to introduce extra degrees of freedom in the model at high slip values, we analyze two add-ons for the model. These are semi-empirical rules and it is no longer a question of Coulomb friction.

2.4.1 Add on-1: Friction dependency on contact Pressure

In rubber friction experiments, it is often observed that the slip friction coefficient μ_{slip} depends on the contact pressure p [17].

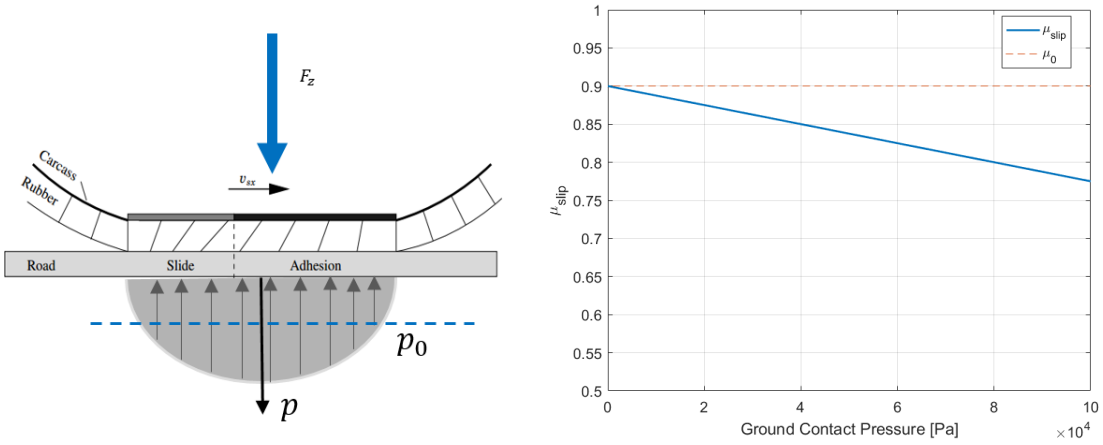

(a) **(b)**

Figure 2.5: (a): Physical model of tyre brush model for pressure distribution, (b): Slip friction co-efficient dependency on Ground pressure

To include this effect, we introduce the following relation $\mu_{slip} = f(p)$, to decrease the slip friction coefficient with increase in pressure in brush elements.

$$\mu_{slip}(\xi) = \mu_0 - \mu_1 \cdot \frac{p(\xi)}{p_0} \tag{2.20}$$

where:
$\mu_0 = \mu_{0,slip} = \frac{\mu_{stick}}{\beta}$
$\mu_1 = 0.05$, tuning constant
$p(\xi) =$ Contact patch pressure at any brush element
$p_0 = 4 * 10^4$ Pa, average of the pressure over the contact patch area

Substituting (2.20) in (2.14) and integrating over the contact patch from $\xi = 0$ to $\xi = L$ gives the a modified brush model expression, check appendix.

This add-on explains the tyre characteristics for varying inflation pressure as in fig 2.6. By increasing the inflation pressure, the contact patch decreases, thereby changing the ground pressure distribution and affecting the slip friction co-efficient at the individual brush elements. This simulation output is more realistic, as you deflate your tyres you get more traction force as explained by the trend in the figure.

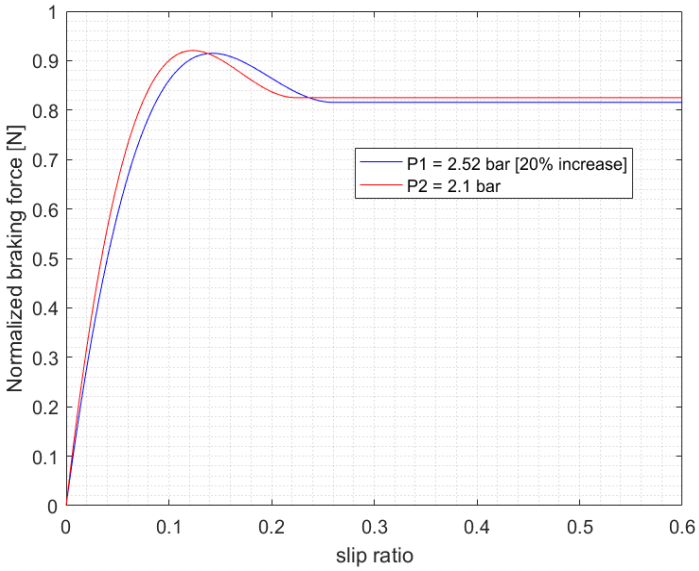

Figure 2.6: Inflation Pressure sensitivity study with add-on

2.4.2 Add-on 2: Friction dependency on slip

The base brush model works good at low slip values and deviate from the results at high slip values. By introducing this add-on the simulation results matches closely with experimental data even at high slips, fig 4.5. To achieve that, we analyze the slip friction co-efficient dependency on slip ratio. It is purely empirical due to lack of sufficient motivation through a physical approach.

We introduce a linear function to study this effect, $\mu_{slip}(s_x) = a + b \cdot s_x$ in the saturation region marked with sticker '2' as shown in fig 2.7. An alternative assumption could have been to assume that friction coefficient varies linearly with sliding speed which is $R \cdot \omega - v_x$.

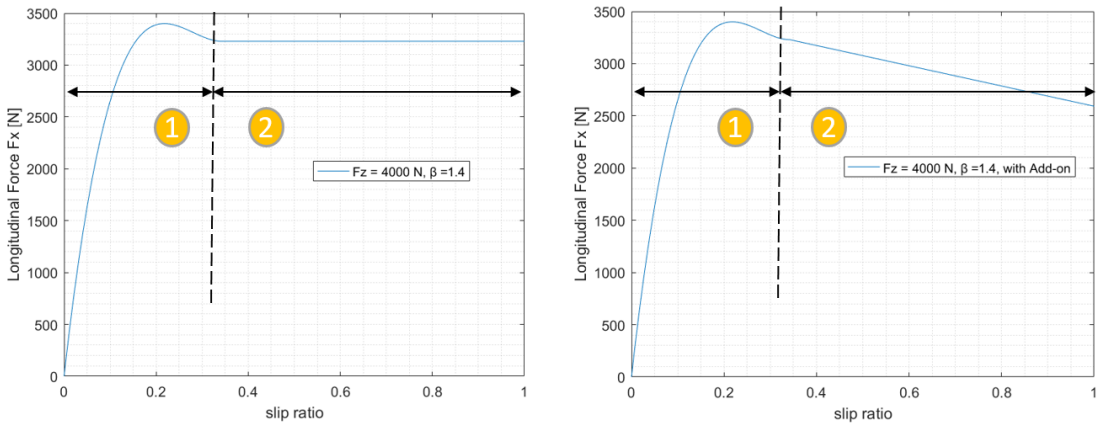

(a) **(b)**

Figure 2.7: (a): Base Brush model, (b): Brush model with Add on-2

The output characteristics with add on activated is approximated more accurately to the measurement data, see fig 4.5. The user has flexibility to run the simulations with or without add ons and also combining the add ons.

2.5 Rolling Resistance Modelling

2.5.1 Spring Damper approach for rolling resistance

Different concepts can be used to model rolling resistance. In this section, rolling resistance is modelled assuming radial spring and damper elements extending from rim to the outer diameter of the tyre throughout the circumference[10]. As shown in figure 2.8, the springs compress upon entering the contact patch and recover while leaving. The energy dissipation occurs in the damper elements and this leads to additional torque requirement for maintaining constant wheel speed.

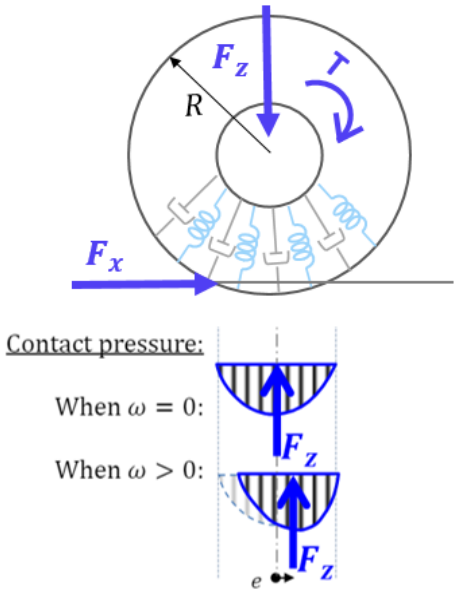

Figure 2.8: Distributed radial springs and dampers in a tyre

The rolling resistance coefficient is defined by

$$rrc = \frac{\frac{T}{R_l} - F_x}{F_z} \tag{2.21}$$

$$rrc = \frac{e}{R} \tag{2.22}$$

where e is the offset distance of reaction force from the centre. It is calculated by taking moment balance about the wheel centre that consists of spring and damper forces.
A friction element is then added to this which is independent of velocity. This gives an explanation for existence of rolling resistance force at zero velocities[19].

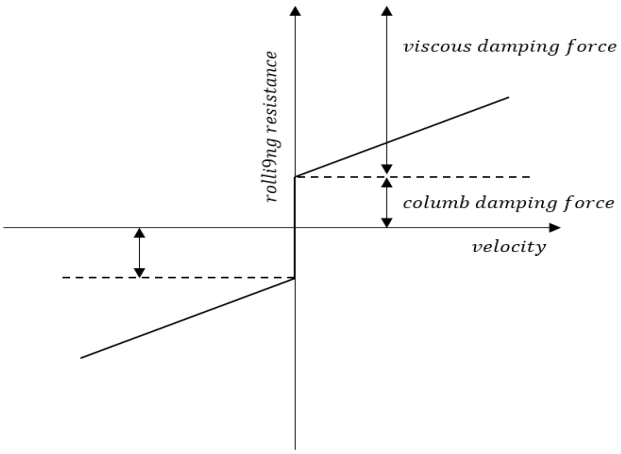

Figure 2.9: Total resistance force offset from the origin as a result of coulumb damping and viscous damping

2.5.2 Momentum transfer approach for rolling resistance

The spring and damper approach discussed earlier manages to explain the relation between rolling resistance and velocity. It also explains rolling resistance at zero velocity through friction element. The drawback with this approach is that the rolling resistance coefficient varies linearly with velocity. It is seen that this is not true in real world scenario where the relation is non-linear.

Another modelling approach for rolling resistance is considered in this section[8]. It explains energy loss as a result of two processes. One is the momentum transfer by the wheel when it encounters the ground when rotating and another is the energy dissipation losses while the tyre is deformed by the ground. This method takes into consideration the material properties of the tyre to determine the amount of equivalent torque loss.

2.5.3 Energy loss due to momentum transfer

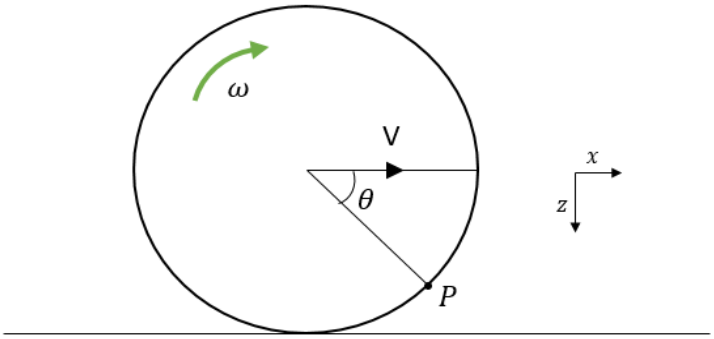

Figure 2.10: tyre on road surface. Co-ordinate system is at rest on the ground.

The rubber mass is rotating with a rotational velocity ω. When it reaches point P, the velocity of this point goes to zero and hence there is momentum transfer from the wheel to the ground.

Consider the figure 2.10 where the wheel axle is moving with speed V relative to the road along the x-axis. The radial thickness of the tyre is ignored here. The point P moves along the circumference of the wheel making an angle θ with the horizontal. Now for a reference frame at rest on the ground, the horizontal and vertical components of the velocity for point P are given by

$$V_x(\theta) = V - V\sin\theta \tag{2.23}$$

$$V_z(\theta) = V\cos\theta \tag{2.24}$$

At $\theta = \frac{\pi}{2}$,these velocities become zero i.e, $V_x = V_z = 0$

Consider the case when the tyre is deformed by the road on contact as shown in figure 2.11.

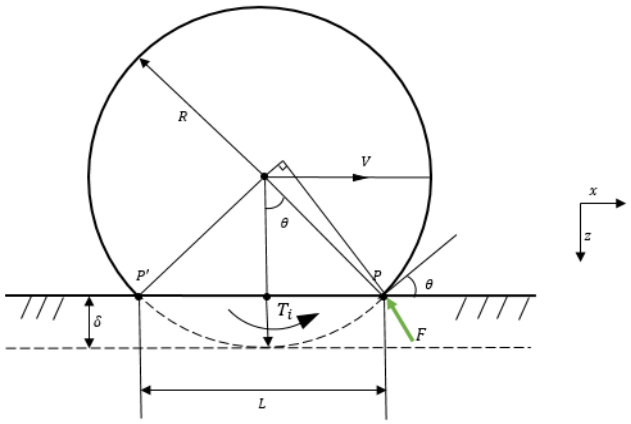

Figure 2.11: tyre deformed by the road surface. Co-ordinate system is on the road surface.

Just before the point P makes contact with the ground, the velocity components are given by

$$V_x(\frac{\pi}{2} - \theta) = V - V\cos\theta \tag{2.25}$$

$$V_z(\frac{\pi}{2} - \theta) = V\sin\theta \tag{2.26}$$

When the point makes contact with the ground, there is momentum transfer between the point and the ground. The horizontal force required for this change in momentum is exerted on the tyre by the road and is given by

$$F_x = \left(\frac{dp}{dt}\right)_x = \dot{m}_t \Delta V_x \tag{2.27}$$

$$F_z = \left(\frac{dp}{dt}\right)_z = \dot{m}_t \Delta V_z \tag{2.28}$$

ΔV = (velocity at time *'t+Δt'*) - (velocity at time *'t'*), which leads to

$$\Delta V_x = V(\cos\theta - 1) \tag{2.29}$$

$$\Delta V_z = -V\sin\theta \tag{2.30}$$

The term $\dot{m}_t$ is the mass flow rate along the circumference and is given by

$$\dot{m}_t = \frac{M_t}{\pi \cdot 2R} \cdot V \tag{2.31}$$

$$T_i = F_x \cdot R \cdot \cos\theta - F_z \cdot \frac{L}{2} \tag{2.32}$$

$$T_i = \frac{m_t \cdot V^2}{2\pi}[1 - \cos\theta] \tag{2.33}$$

The power required to compensate for the torque loss is given by

$$P_t = \frac{V}{R} \cdot T_i \cdot \varepsilon_t \tag{2.34}$$

Where ε_t determines the elasticity of the tyre i.e, $\varepsilon = 1$ means that the tyre is completely plastic during impact with ground and $\varepsilon_t = 0$ means the tyre is perfectly elastic and there is no loss. The rolling resistance force generated corresponding to this loss is given by

$$Fr_{impact} = \frac{P_t}{V} \tag{2.35}$$

Another interpretation of this phenomenon is that the impact force will result in a skewed pressure distribution towards the inlet side of the contact. This will result in an equivalent torque loss. This impact torque can then be represented as

$$T_i = \frac{P_t}{\omega} \tag{2.36}$$

2.5.4 Energy loss due to flexing

This part of the energy loss assumes that the work done during deformation of the tyre from the point $x = 0$ to the point $x = L/2$ is not recovered completely from the point $x = L/2$ to the point $x = L$ and there is energy being lost here in the form of mechanical dissipation in the form of heat and noise.

The work per revolution to flex the tyre is given by the equation

$$W_f = \frac{2\pi}{\theta} \cdot P \cdot W \cdot \int_0^{\frac{L}{2}} \delta_z \cdot dx \tag{2.37}$$

where P is the constant ground pressure on the tyre.

$$W_f = \frac{2\pi}{\theta} \cdot \frac{P \cdot W}{2}\Big[\pi \cdot R^2 \cdot \frac{\theta}{\pi} - \Big(R - \delta\Big)\frac{L}{2}\Big] \tag{2.38}$$

The corresponding power to flex the tyre is the calculated with

$$P_f = \frac{V}{R} \cdot W_f \cdot \varepsilon_f \tag{2.39}$$

The rolling resistance force generated corresponding to this loss is given by

$$Fr_{flex} = \frac{P_f}{V} \tag{2.40}$$

The total rolling resistance force is given by adding equations 2.35 and 2.40

$$Fr = Fr_{impact} + Fr_{flex} \tag{2.41}$$

$$Fr = \left(\frac{m_t}{2\pi \cdot R}[1 - \cos\theta] \cdot \varepsilon_t\right) \cdot V^2 + \left(\frac{\varepsilon_f}{R}\frac{2\pi}{\theta} \cdot \frac{P \cdot W}{2}\left[\pi \cdot R^2 \cdot \frac{\theta}{\pi} - \left(R - \delta\right)\frac{L}{2}\right]\right) \tag{2.42}$$

At V=0, the velocity dependent term Fr_{impact} becomes zero but the velocity independent term Fr_{flex} still exists giving an offset at the origin.

3

Soft Surface

3.1 Introduction

Soil-wheel interaction on soft surfaces is often not modeled due to the complex nature of such an interaction. Factors like the rolling resistance and braking force vary significantly compared to hard surfaces which leads to a higher energy consumption. There is a need to capture the mechanics of this interaction for off-road vehicles or passenger cars travelling over soft surfaces. The significant difference in this case compared to hard surface is that the wheel sinks into the ground and this sinkage depends on the surface properties as well as geometric properties of the wheel. The model becomes more complex when factors of velocity dependence and inflation pressure dependence are included. The efforts of many researchers on this subject are explored and an attempt is made to develop a single model to predict the main features of a tyre operating in off-road scenarios[2,3,6,7,9,11,12,14].

3.1.1 Bekker's sinkage theory

The approached used in this project for modelling soft soil mechanics is an extension of Bekker's sinkage theory. Bekker M.G. proposed a formulation that relates the sinkage height of a static plate of width b on deformable soil and the normal pressure it experiences because of the force applied to it as seen in fig 3.1 [2]. It was seen that the relation is of a non-linear nature because of soil compaction with increased normal load.

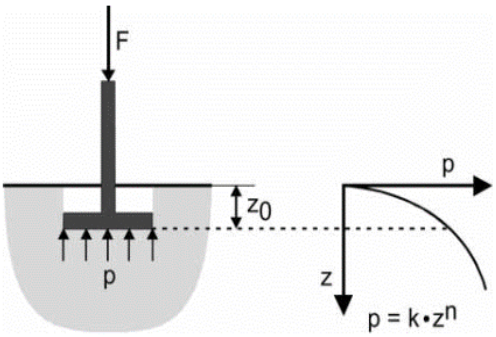

Figure 3.1: Plate pressed against deformable ground, (b): pressure vs sinkage curve [3]

Bekker's sinkage equation is based on experimental data that includes various surface properties. It is given by:

$$P(z) = k \cdot z^n = (\frac{k_1}{b} + k_2) \cdot z^n \tag{3.1}$$

where k_1, k_2 and n are termed as pressure-sinkage parameters and determined by plate sinkage tests. This equation has played a vital role in developing tyre models for vehicle terrain interaction for off road applications.

The model presented in the thesis works includes both rigid tyres and flexible tyres. The rigid wheel can be assumed as a first approximation of flexible tyre.

3.2 Rigid Wheel Model

This model assumes tyre as a rigid wheel especially when the surface is softer than the tyre resulting in more significant deformation of the terrain than the tyre itself provided a minimum tyre inflation pressure is maintained. Another scenario when this assumption holds true is when the tyre is inflated to a point where the combined pressure of the stiff carcass and the inflation pressure exceed the load bearing capacity of the terrain.

Reece [11] and Karafiath [12] asserted that equation 3.1 is inconsistent with the perception from bearing capacity theory and later modified to :

$$P(z) = (ck_1^{'} + b\gamma k_2^{'})\Big(\frac{z}{b}\Big)^n \tag{3.2}$$

where P is the pressure in Pa, z is the sinkage in m, c is the cohesion of the soil in Pa, $k_1^{'}$ and $k_2^{'}$ are modified from equation 3.1 by introducing $(\frac{z}{b})$ so that the quantities k_1 and k_2 become dimensionless, b is a width of the tyre in m, n is the sinkage exponent and γ is the weight density of soil in N/m^3.

3.2.1 Bekker's theory applied to wheels

The same principle can be extended to a wheel that is sinking in the ground. There can be two cases, one where the wheel is static on the soil surface as seen in fig 4.20a and one where the wheel is moving with a velocity of ω on the soil surface as seen in fig 4.20b.

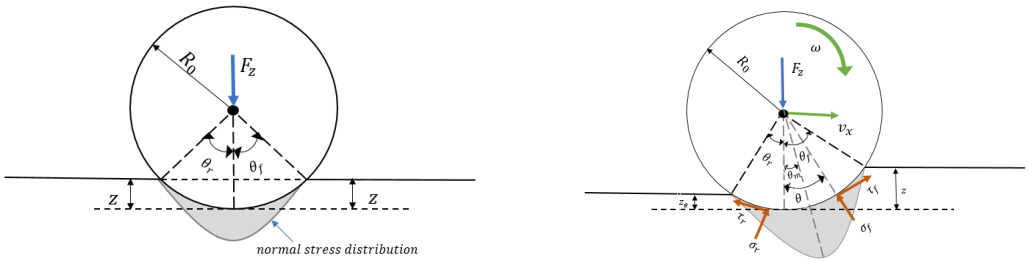

(a) **(b)**

Figure 3.2: (a): Static wheel on soft soil (b): Rotating wheel on soft soil

In the first case where the wheel is static, the height of the soil in front of the wheel is the same as behind the wheel making the entry angle θ_f and exit angle θ_r equal. The normal load distribution is symmetric about the wheel centre. The second case however is more complicated as the wheel moves forward which makes the soil height at the point of entry higher than the height at the point of exit. The entry and exit angles have different values and the normal load distribution is skewed. The point at which the load distribution is maximum is extended to the wheel centre and the angle between this line and the centre line is termed as θ_m. For any arbitrary angle θ, it can be seen from geometry that

$$z(\theta) = R_0(\cos\theta - \cos\theta_f) \tag{3.3}$$

3.2.2 Enhanced Bekker's Model

The Bekker equation 3.2 applied to wheels is the basis for the modeling approach used in this thesis [3]. The skewed load distribution in the contact area gives rise to normal stress and shear stress along the entire contact patch as seen in figure 3.2b.

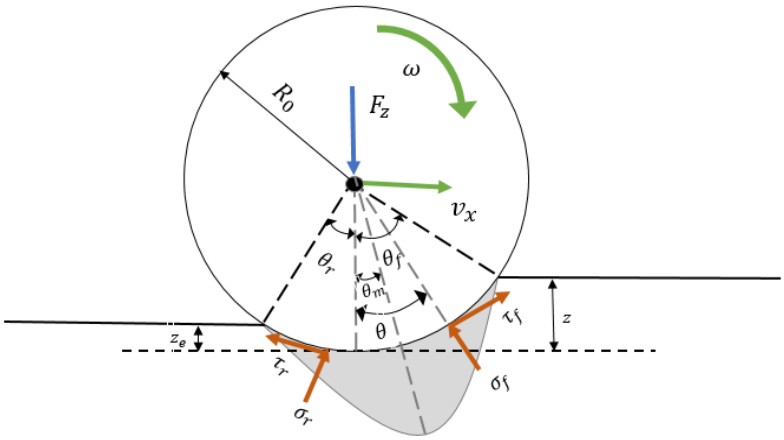

Figure 3.3: Soft surface model simulation result, typical tyre characteristics in deformable ground

The relation between different angles in the figure are expressed below
It is assumed that the exit angle is a fraction of the entry angle. θ_m is the angle where the maximum normal stress is acting on the wheel. θ_m is expressed using a relation that is proportional to longitudinal slip and empirical constants that have been successfully implemented before [13,14,15]. The equations are shown below.

$$\theta_r = i\theta_f \tag{3.4}$$

$$\theta_m = (c_0 + c_1 s_x)\theta_f \tag{3.5}$$

The expression for normal stress and shear stress are given below [3]

for $\theta_m < \theta < \theta_f$,

$$\sigma_f(\theta) = (c \cdot k_1 + b\gamma k_2)\left(\frac{R_0}{b}\right)^n (\cos(\theta) - \cos(\theta_f))^n \tag{3.6}$$

for $\theta_r < \theta < \theta_m$,

$$\sigma_r(\theta) = (c \cdot k_1 + b\gamma K_2)\left(\frac{R_0}{b}\right)^n \left(\cos\left(\theta_f - \frac{(\theta - \theta_r)}{(\theta_m - \theta_r)}(\theta_f - \theta_m)\right) - \cos(\theta_f)\right)^n \tag{3.7}$$

The verticals component of the normal stress is given by

$$F_{z_\sigma} = R_0 b\left(\int_{\theta_f}^{\theta_m} \sigma_f \cos(\theta) d\theta + \int_{\theta_m}^{\theta_r} \sigma_r \cos(\theta) d\theta\right) \tag{3.8}$$

The expression for shear stress beneath the wheel is based upon empirical calculations first introduced by Janosi and Hanamoto[21] and widely used:

$$\tau_f(\theta) = \tau_{f_{max}}\left(1 - e^{\frac{-J_x}{k_x}}\right) \tag{3.9}$$

$$\tau_r(\theta) = \tau_{r_{max}}\left(1 - e^{\frac{-J_x}{k_x}}\right) \tag{3.10}$$

where,
limiting shear stress:

$$\tau_{f_{max}} = c + \sigma_f(\theta) tan\phi \tag{3.11}$$

$$\tau_{r_{max}} = c + \sigma_r(\theta) tan\phi \tag{3.12}$$

shear displacement of the terrain:

$$J_x = R_0(\theta_f - \theta - (1 - s_x)\sin\theta_f - \sin\theta) \tag{3.13}$$

and shear deformation modulus: k_x

The verticals component of the shear stress is given by

$$F_{z_\tau} = R_0 b \left(\int_{\theta_f}^{\theta_m} \tau_f \sin(\theta) d\theta + \int_{\theta_m}^{\theta_r} \tau_r \sin(\theta) d\theta \right) \tag{3.14}$$

The total load $'F_z'$ on the tyre is balanced with the vertical components given by equations (1.8) and (1.14)

$$F_z = F_{z_\sigma} + F_{z_\tau} \tag{3.15}$$

The only unknown in the set of equations leading to 1.15 is the entry angle of the wheel θ_f.The model calculates this value through multiple iterations to match the vertical load.

The obtained value for the angle is substituted in the equation below to find out the horizontal force component F_x.

$$F_{x_\sigma} = R_0 b \left(\int_{\theta_f}^{\theta_m} \sigma_f \sin(\theta) d\theta + \int_{\theta_m}^{\theta_r} \sigma_r \sin(\theta) d\theta \right) \tag{3.16}$$

$$F_{x_\tau} = R_0 b \left(\int_{\theta_f}^{\theta_m} \tau_f \cos(\theta) d\theta + \int_{\theta_m}^{\theta_r} \tau_r \cos(\theta) d\theta \right) \tag{3.17}$$

$$F_x = F_{x_\sigma} + F_{x_\tau} \tag{3.18}$$

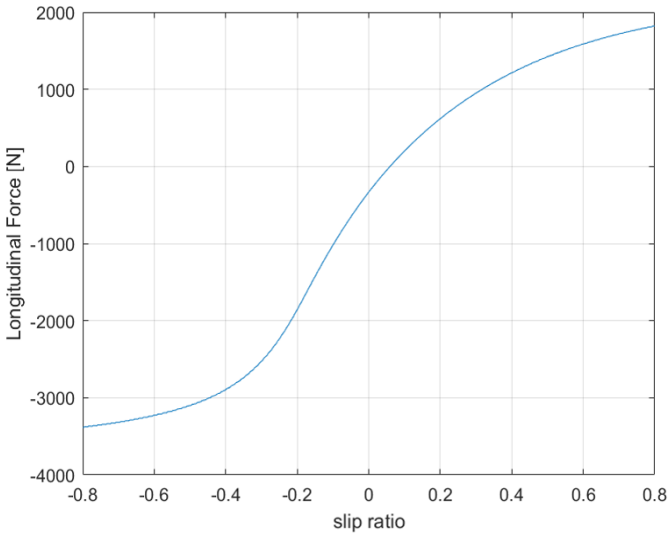

Figure 3.4: Soft surface model simulation result, typical tyre characteristics in deformable ground plotted for $v_x = 5.5m/s$ and $F_z = 4000N$

The F_{x_σ} part in the equation 3.18 constitutes the rolling resistance for this model. In other words, it is viewed as a part of the total horizontal force on the tyre and no further modeling is required. It is seen that there is an offest at origin in the plot 3.4 which is the rolling resistance.

3.2.3 Model with velocity influence

The base model discussed in 3.2.2 does not take velocity of the vehicle into account. It has been suggested in paper [6] that traction force and rolling resistance is dependent on wheel speed. This section provides a velocity dependence to the base model that may be used if necessary. These equations represent a general trend in comparison to the results from the paper [7] but were not validated with test data. However, the empirical parameters may be tuned to match with experimental data when available.

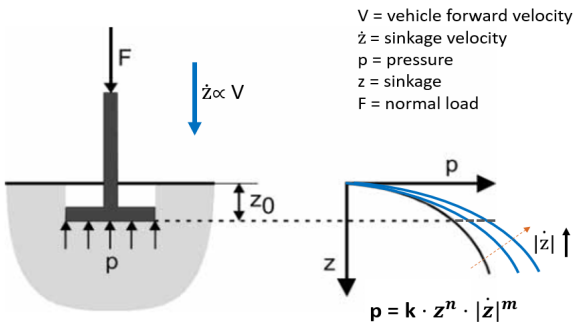

Figure 3.5: Influence of velocity to the sinkage tests

The new equation is an extension of the base model with additional empirical parameters.The only equations that are different from the base model are

for $\theta_m < \theta < \theta_f$,

$$\sigma_f(\theta) = (ck_1 + b\rho k_2)\left(\frac{R}{b}\right)^n (\cos(\theta) - \cos(\theta_f))^n \left(\left(\frac{v_x}{1 - v_x}\right)\sin(\frac{\theta}{v_0})\right)^m \tag{3.19}$$

for $\theta_r < \theta < \theta_m$,

$$\sigma_r(\theta) = (ck_1 + b\rho k_2)\left(\frac{R}{b}\right)^n \left(\cos\left(\theta_f - \frac{(\theta - \theta_r)}{(\theta_m - \theta_r)}(\theta_f - \theta_m)\right) - \cos(\theta_f)\right)^n \left(\left(\frac{v_x}{1 - v_x}\right)\sin(\frac{\theta}{v_0})\right)^m \tag{3.20}$$

The constant 'm' is tuned to obtain plot curves for varying velocity. Comparison of plots with and without velocity dependence are done in the later parts of the report.

4

Validation & Results

4.1 Hard Surface

4.1.1 $F_x(s_x)$ Validation

There are two ways in which the model is validated in the following sections. Sections 4.1.1.1 to 4.1.1.3 are validated by checking the model behaviour qualitatively to see if the model follows the desired direction/trend by changing a single design parameter or operating condition at a time. Section 4.1.1.4 is validated by taking existing data for a particular tyre and tuning the empirical parameters of the model.

4.1.1.1 Requirements

In instances where data is missing to validate the tyre model, One way is to check if it meets the requirements on model. These requirements are proposed by vehicle dynamic researchers based on experience and found to be true for well known magic formula. The requirements of a model on hard surface are:

1. For increasing F_z, the slip where $F_{x,peak}$ occurs should slightly increase $\frac{\partial s_{x,peak}}{\partial F_z} > 0$
2. For increasing F_z, the $F_{x,peak}$ should increase almost proportional to Fz, but degressively $\frac{\partial F_{x,peak}}{\partial F_z} > 0, \frac{\partial^2 F_{x,peak}}{\partial F_z^2} \leq 0$
3. For increasing F_z, the longitudinal stiffness C_x should increase almost proportionally, but degressively $\frac{\partial C_x}{\partial F_z} > 0, \frac{\partial^2 C_x}{\partial F_z^2} < 0$
4. For increasing $P_{inflation}$, the rolling resistance coefficient should decrease $\frac{\partial rrc}{\partial P_{infl}} < 0$

5. The model should be possible to verify experiment data

4.1.1.2 Requirements verification

Simulation output behaviour
The simulation results of the tyre-brush model are in agreement with the requirements listed in previous section. The fig 4.1 explains the requirements 1 to 3 listed

in 4.1.1.1 and the fig 4.2 explains the requirement 4. The longitudinal stiffness C_x is initial slope of the curve.

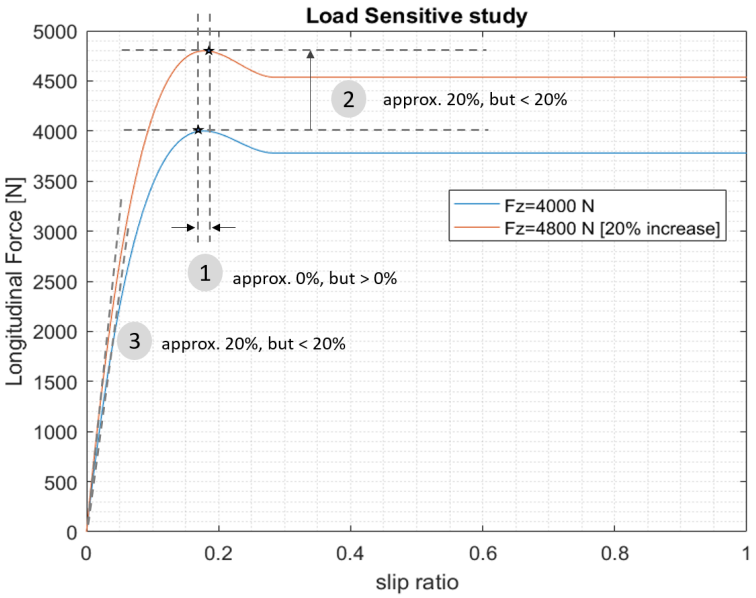

Figure 4.1: Simulation results in agreement with the requirement points 1 to 3 for the Hard surface model

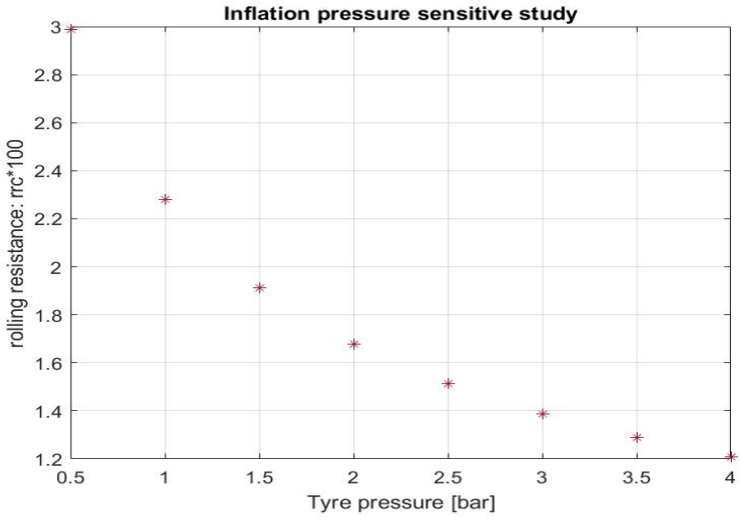

Figure 4.2: Simulation result in agreement with the Requirement 4 for the Hard surface model

Mathematical derivations
This section shows a mathematical proof to show the tyre-brush model meets the proposed requirements.
Revisiting to the modified brush model equation:

$$F_x \cdot sgn(s_x) = \begin{cases} \mu_{slip} \cdot F_z & \text{if } \omega \cdot v_x < 0 \\ C_x \cdot |s_x| - (2 - \frac{\mu_{slip}}{\mu_{stick}}) \cdot \frac{(C_x \cdot |s_x|)^2}{3 \cdot \mu_{stick} \cdot F_z} + (3 - 2\frac{\mu_{slip}}{\mu_{stick}}) \cdot \frac{(C_x \cdot |s_x|)^3}{27 \cdot (\mu_{stick} \cdot F_z)^2} & \text{else if } |s_x| < \frac{3\mu_{stick} \cdot F_z}{C_x} \\ \mu_{slip} \cdot F_z & \text{else} \end{cases} \tag{4.1}$$

Requirement 1 : Peak Slip Location, $s_{x,peak}$

The slip value at which the force peak occurs is derived as follows:

$$\frac{\partial F_x}{\partial s_x} = 0 \quad \Rightarrow \quad s_{x,peak} = \frac{3 \cdot \mu_{stick} \cdot F_z}{C_x \cdot (3 - 2\frac{\mu_{slip}}{\mu_{stick}})}; \qquad if \quad |s_x| < \frac{3 \cdot \mu_{stick} \cdot F_z}{C_x} \tag{4.2}$$

$$\frac{\partial s_{x,peak}}{\partial F_z} = \frac{3 \cdot \mu_{stick} \cdot F_z}{C_x \cdot (3 - 2\frac{\mu_{slip}}{\mu_{stick}})}; \qquad (> 0, \ as \ C_x > 0 \ and \ \mu_{stick} \geq \mu_{slip}) \tag{4.3}$$

Requirement 2 : Influence of F_z **on** $F_{x,peak}$

Substituting eq 2 in 1 with s_x as $s_{x,peak}$

$$\begin{aligned} F_{x,peak} = C_x \cdot |\frac{3 \cdot \mu_{stick} \cdot F_z}{C_x \cdot (3 - 2\frac{\mu_{slip}}{\mu_{stick}})}| - (2 - \frac{\mu_{slip}}{\mu_{stick}}) \cdot \frac{(C_x \cdot |\frac{3 \cdot \mu_{stick} \cdot F_z}{C_x \cdot (3 - 2\frac{\mu_{slip}}{\mu_{stick}})}|)^2}{3 \cdot \mu_{stick} \cdot F_z} \\ + (3 - 2\frac{\mu_{slip}}{\mu_{stick}}) \cdot \frac{(C_x \cdot |\frac{3 \cdot \mu_{stick} \cdot F_z}{C_x \cdot (3 - 2\frac{\mu_{slip}}{\mu_{stick}})}|)^3}{27 \cdot (\mu_{stick} \cdot F_z)^2}; \end{aligned} \tag{4.4}$$

$$\begin{aligned} \frac{\partial F_{x,peak}}{\partial F_z} = |\frac{3 \cdot \mu_{stick}}{(3 - 2\frac{\mu_{slip}}{\mu_{stick}})}| - (2 - \frac{\mu_{slip}}{\mu_{stick}}) \cdot \frac{|\frac{3 \cdot \mu_{stick}}{(3 - 2\frac{\mu_{slip}}{\mu_{stick}})}|)^2}{3 \cdot \mu_{stick}} \\ + (3 - 2\frac{\mu_{slip}}{\mu_{stick}}) \cdot \frac{(|\frac{3 \cdot \mu_{stick}}{(3 - 2\frac{\mu_{slip}}{\mu_{stick}})}|)^3}{27 \cdot (\mu_{stick})^2}; \quad (> 0, \mu_{stick} \geq \mu_{slip}) \end{aligned} \tag{4.5}$$

Independent of C_x and F_z

$$\frac{\partial^2 F_{x,peak}}{\partial F_z^2} = 0 \tag{4.6}$$

4.1.1.3 Tyre-Brush Model Behaviour

The typical model behaviour for different surfaces can be seen in fig 4.3.

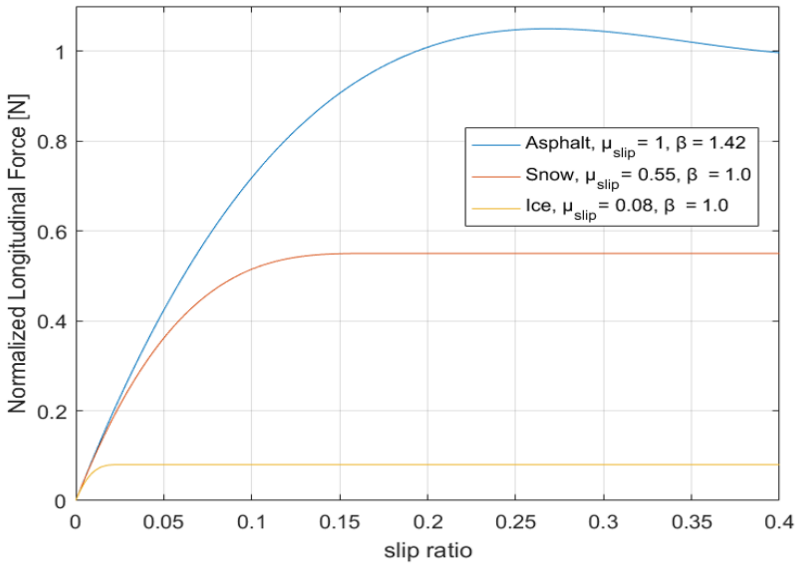

Figure 4.3: General characteristics of tyre curves generated for surfaces - asphalt, snow and ice covered

4.1.1.4 Validation of tyre-brush model with measured data

This section shows some of the validation results for all three type of Summer, Winter and studded tyres majorly on wet asphalt road surface. All the measured data is taken from VTI [17]. The calibration factor β used for simulations in wet asphalt and snow is 1.4 and 1.2 respectively throughout this section.

Summer tyres

Continental tyre ContiSportContact, 225/45R17 is used for measurements. The fig 4.4 shows the comparison of Simple brush model results with measurement data at a load of 4000 N on wet asphalt surface. It shows that base brush model shows close approximation to the measurement data at low slips and deviates at high slips.

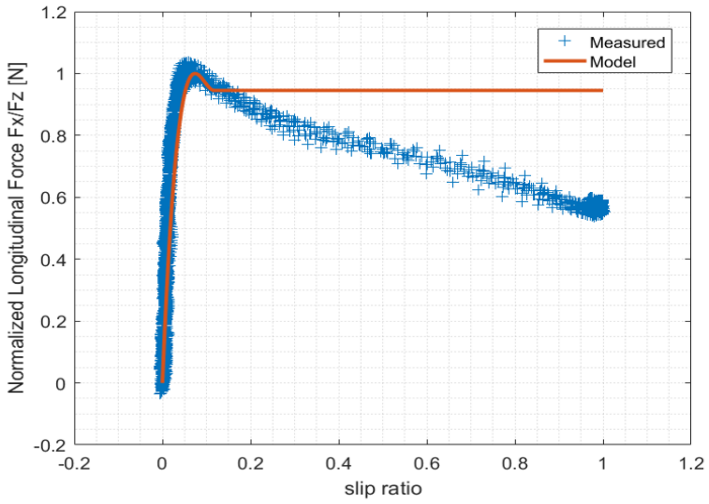

Figure 4.4: Validation plot for $F_z = 4000$ N, $v_x = 60$ km/h, wet asphalt, Summer tyre, Simple brush model

To make the vehicle dynamic simulations more flexible and accurate in the entire range of slip values, we activate the add on-2. Comparison with add on is shown in fig 4.5, where the slope of the line in region '2' is adjusted to the slope of measurement data.

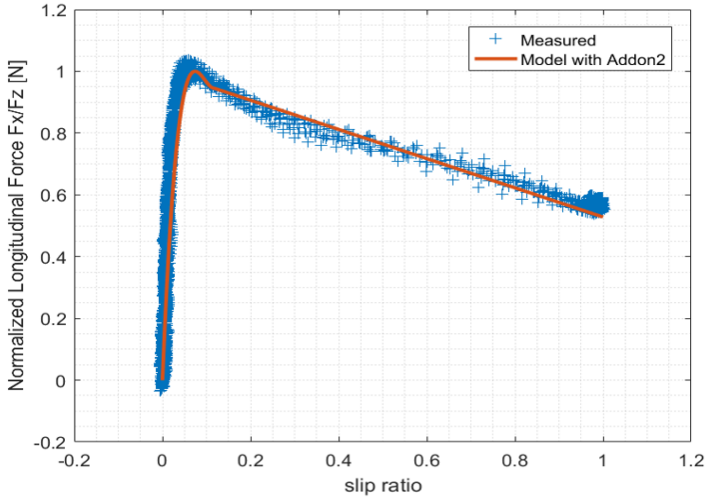

Figure 4.5: Validation plot for $F_z = 4000$ N, $v_x = 60$ km/h, wet asphalt, Summer tyre, Brush model with add-on2

Winter tyres

Continental tyre ContiWinterContact 215/55R16 is used for all the measurements in this sub section. The fig 4.6 shows the comparison of Base brush model results with measurement data at a load of 4000 N, on snow surface. For snow conditions the base brush model gives good approximations over entire range of slip values as the force value fairly remains constant in the saturation

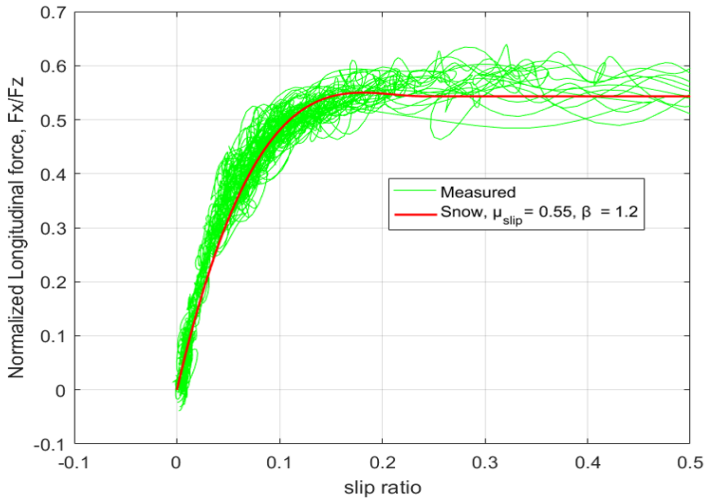

Figure 4.6: Validation plot for $F_z = 4000$ N, $v_x = 60$ km/h, snow, Winter tyre, Simple brush model

The fig 4.7 show the comparison plot on wet asphalt with base brush model, which approximates the measurement data till the peak and drop down at low slip values.

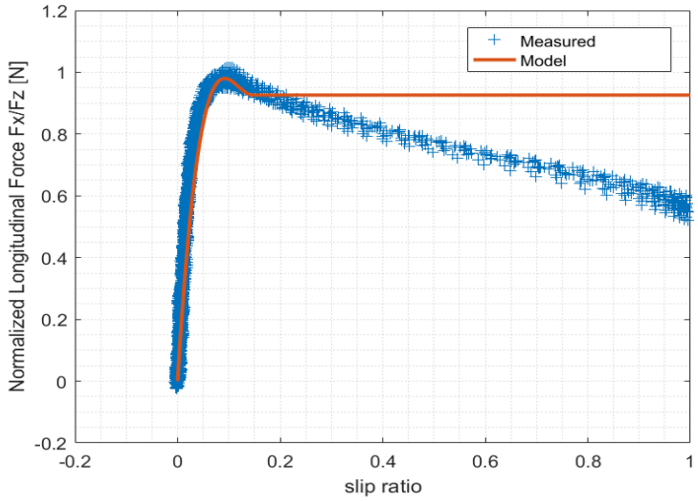

Figure 4.7: Validation plot for $F_z = 4000$ N, $v_x = 60$ km/h, wet asphalt, Winter tyre, Simple brush model

The model is made flexible at high slips by activating the add on-2 and the results are shown in fig 4.8

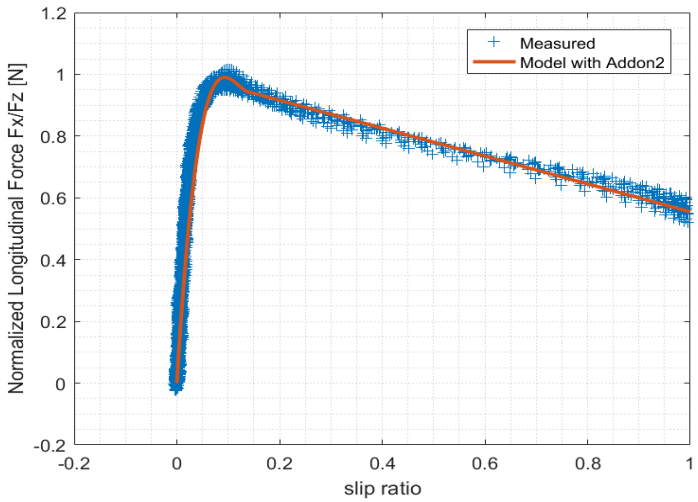

Figure 4.8: Validation plot for $F_z = 4000$ N, $v_x = 60$ km/h, wet asphalt, Winter tyre, Brush model with add on-2

Studded tyres

Gislaved Nordfrost 3, 215/55R16 tyre is used for all measurement data in this sub section. Similarly to summer and winter tyres, the base brush model gives good approximation at low slip values and activating the add on-2 gives better approximation at high slips. The results are depicted in 4.9 for base model and 4.10 for the model with add on.

For the cases where pure physical approach is desired, one can use the base brush model which gives good approximation of the model till the saturation is reached. Most of the vehicle dynamic simulations are performed for low slip conditions and the base model gives good results.

The model with add ons gives the user more flexibility to run the simulations in entire slip ranges by adjusting some empirical constants. To conclude, the improved brush model is flexible for the user as per the requirements.

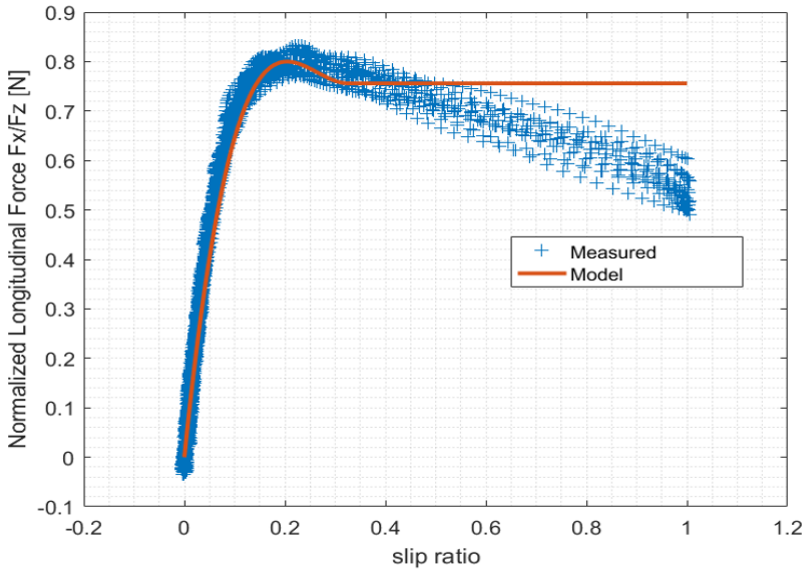

Figure 4.9: Validation plot for $F_z = 4000$ N, $v_x = 60$ km/h, wet asphalt, Studded tyre, Simple brush model

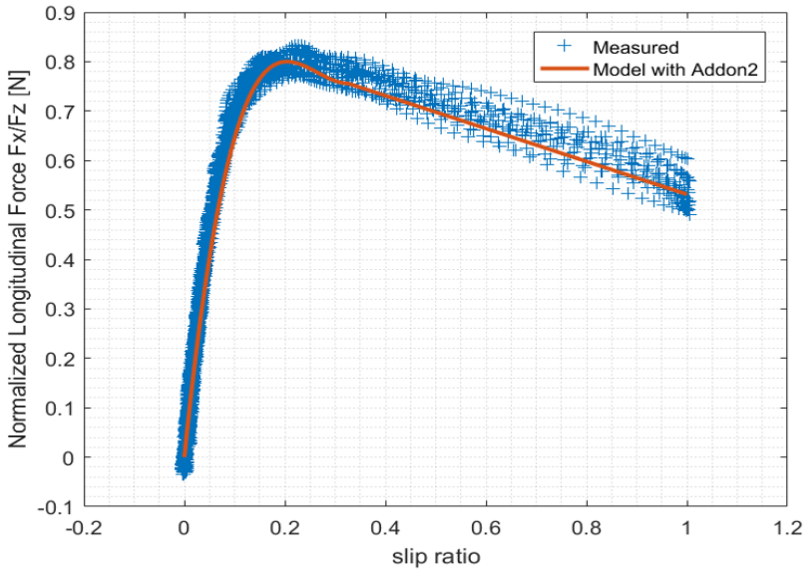

Figure 4.10: Validation plot for $F_z = 4000$ N, $v_x = 60$ km/h, wet asphalt, Studded tyre, Brush model with add on-2

4.1.2 Rolling Resistance validation

4.1.2.1 Requirements for rolling resistance model

Certain criteria are expected to be met by the rolling resistance model based on previous researches and general trends observed in measurement data. This provides a good base to validate the model when obtaining experimental data is difficult. The main requirements for the rolling resistance model are listed below continuing to the list from the 4.1.1.1.

6. Rolling resistance coefficient varies quadratically with vehicle velocity from its value at zero velocity.
7. There is a non-zero value for rolling resistance coefficient at zero velocity.

4.1.2.2 Rolling Resistance behaviour

This report considers the rolling resistance model discussed in the section 2.5.2. There are two empirical factors which we can vary to adjust the results with measured data. Model tunability is shown in the figure below with three curves by changing one of the empirical factors on each of the figures.

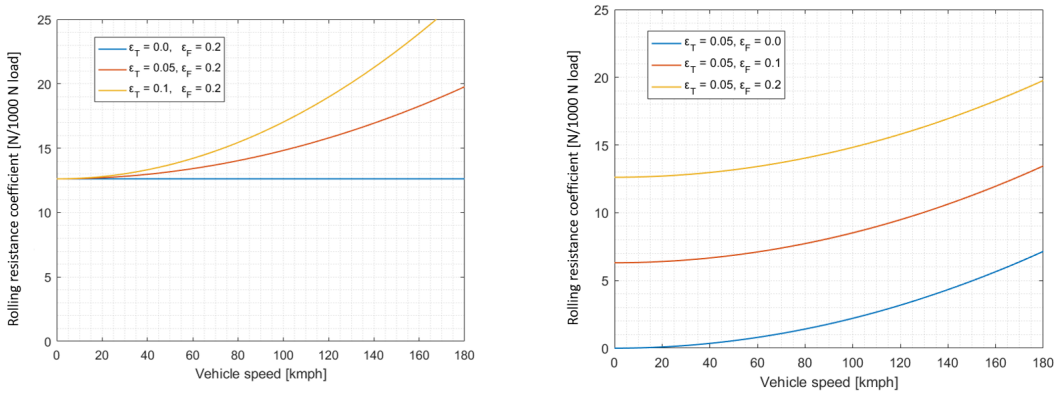

(a) **(b)**

Figure 4.11: Rolling Resistance model tunability with changing only one of the empirical factors in each plot (a): varying ε_T (b): varying ε_F

The nature of the equation that defines rolling resistance is of the form

$$rrc \propto 1 + V^2 \tag{4.7}$$

The figure to the left (4.11 (a)) is the simulation result obtained by varying only the factor ε_T. We see that this affects the curvature of the plot as this factor is associated with the quadratic term in the equation that defines rolling resistance. There is a constant value set for ε_F which gives an offset to the curve.
The figure on the right (4.11 (b)) is the simulation result obtained by setting the factor ε_F as 0 for the blue curve. This makes the offset from origin to become zero. Validation of the model with actual measured data is shown in the figure 4.12.

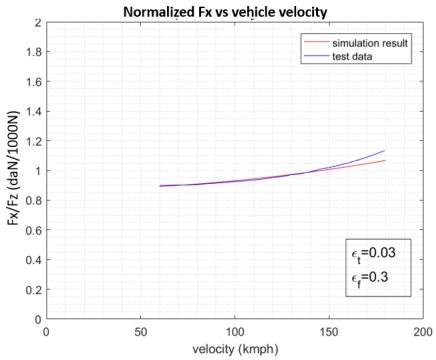

(a) Comparison to data from Michelin 185/65 R15 MXL

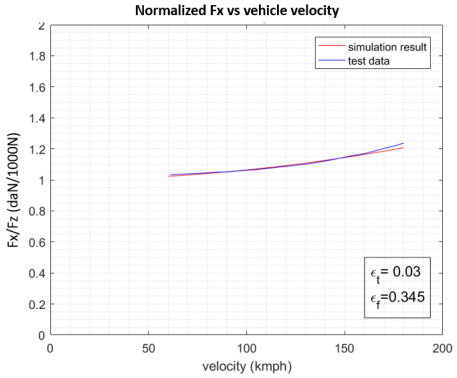

(b) Comparison to data from Michelin 185/65 R15 MXV

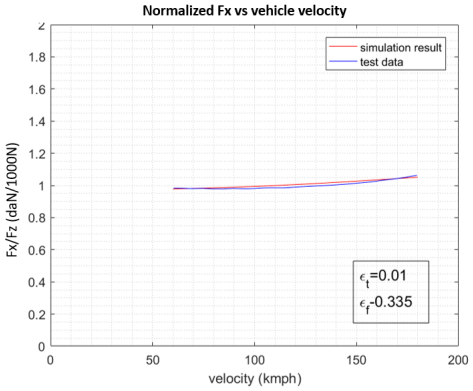

(c) Comparison to data from Michelin 195/60 R15 MXV

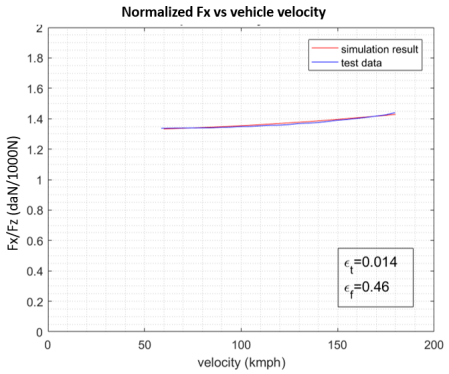

(d) Comparison to data from Michelin 205/50 VR16 MXW

Figure 4.12: Comparison of model output and experimental tyre rolling resistance data at zero input torque

The model result was compared with test data from old tyres of different geometries and different attributes as shown in the figure 4.12. It is seen that the model is capable of replicating the shape of the curve well. The different values for the tuned empirical constants ε_T and ε_F using least square fit are tabulated in table 4.2.

Tyre size	ε_T	ε_F
185/65 R15 MXL	0.03	0.3
185/65 R15 MXV	0.03	0.35
195/60 R15 MXV	0.01	0.335
205/50 VR16 MXW	0.015	0.45

Table 4.1: Values of tuning factors for rolling resistance simulation curves

It should be noted that the data used here are for old tyres and are not representative of tyres on modern cars. The values of ε_T and ε_F may change significantly for modern tyres.
The values of ε_T and ε_F depend on tyre geometric properties and material properties. As seen in fig 4.12 (a) there is a higher curvature compared to fig 4.12 (c). The tyre dimensions in these two cases differ largely. Depending on the build of the tyre(race tyre, passenger tyre), the tuning constants can be generalized and assumed to lie in a range. The magnitude of change in the results for these varying parameters are studied here.

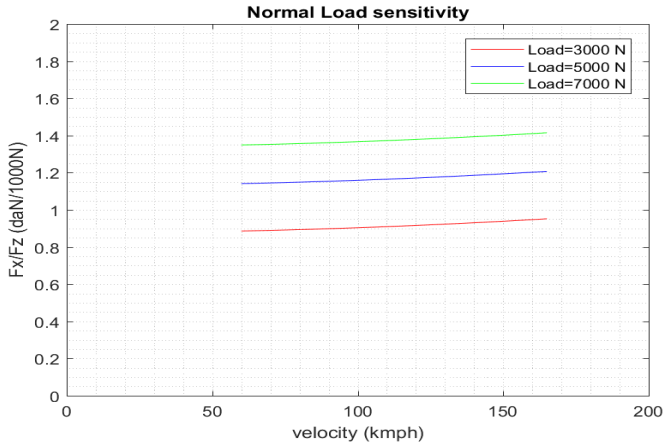

Figure 4.13: sensitivity of the model to changes in normal load by keeping geometric and physical parameters constant.

It is seen that the rolling resistance coefficient increases with increase in normal load. The increase in normal load causes an increase in the contact patch length. This leads to an increase in the work done due to flexing as seen in the equation 2.38. Although, we do not have an explicit requirement on how rolling resistance coefficient should vary with F_z, others have come to opposite conclusion [22].

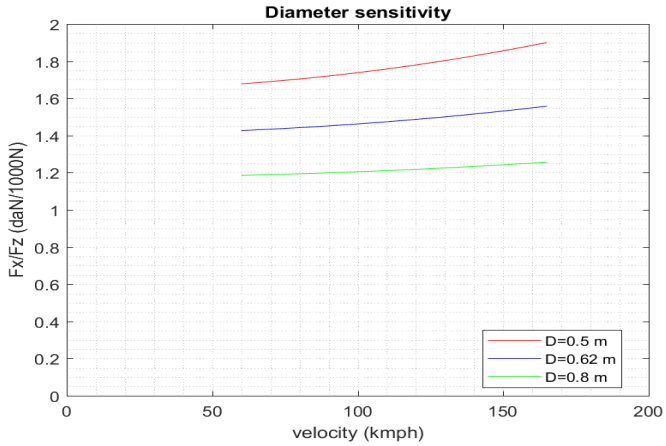

Figure 4.14: Sensitivity of the model to changes in tyre diameter keeping all other geometric and physical parameters constant at a constant normal load.

It is seen that the rolling resistance decreases with increase in diameter and tyre width. The vertical stiffness of the tyre 'K_z' is proportional $\sqrt{diameter * width}$ of the tyre. This means thas for higher values of diameter and width, the vertical stiffness increases. A stiffer tyre implies that the flexing of tyre is reduced which minimizes the flexing losses thereby giving a lower value of rolling resistance.

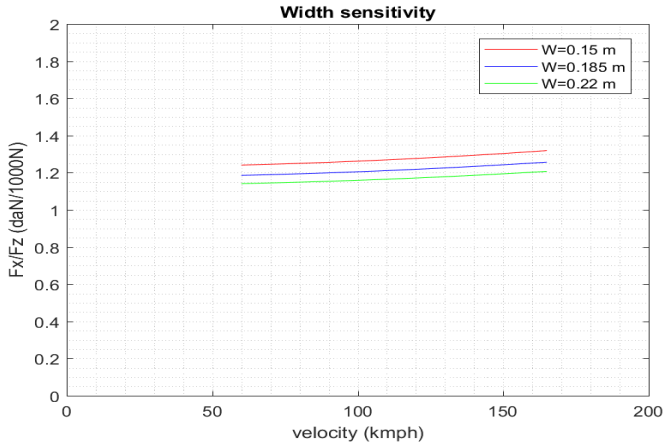

Figure 4.15: Sensitivity of the model to changes in tyre width keeping all other geometric and physical parameters constant at a constant normal load

From figure 4.15 one can see that rolling resistance coefficient decreases with increasing width. However we do not have an explicit requirement on its nature, there are different conclusions [10,22].

It is seen that the tyre mass has lesser effect on rolling resistance at lower velocities but has an increasing trend with increase in mass. The momentum stored in the tyre increases with increase in mass and there is a higher loss in the amount of energy transferred to the ground which can be seen in the equation 2.33

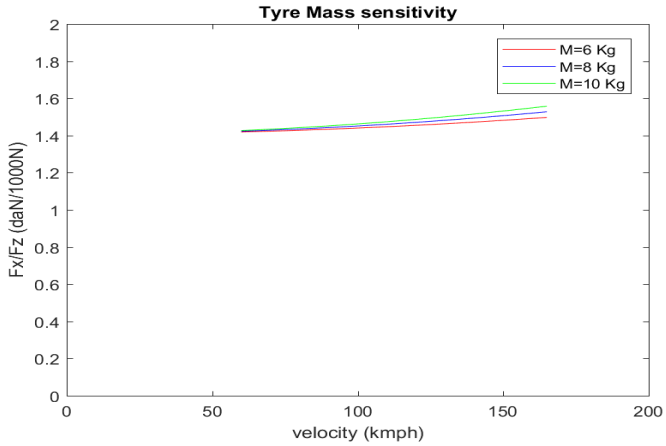

Figure 4.16: Sensitivity of the model to changes in tyre mass which directly co-relates to rubber density by keeping geometric and physical parameters constant at a constant normal load.

4.2 Soft Surface Validation

4.2.1 Requirements on the model - Soft Surface

Similar to the hard surface case, the following requirements should be true for soft surface tyre models. Based on the experience the following have been suggested:

1. Sinkage of wheel decreases with increase in vehicle velocity
2. Longitudinal force decreases with increase in vehicle velocity
3. Rolling resistance force decreases with decrease in sinkage
4. Rolling resistance force increase with increase in vehicle velocity at the same sinkage level

The model proposed in this report is found to be consistent with the listed requirements.

4.2.2 Enhanced bekker model Behaviour

The validation plots presented in the following section are performed using surface properties for dry sand.

Sinkage

The sinkage depth is seen to be reducing with increasing velocities. The wheel does not get enough time to sink into the sand at higher velocities thereby 'skimming' on the soft surface at higher speeds.

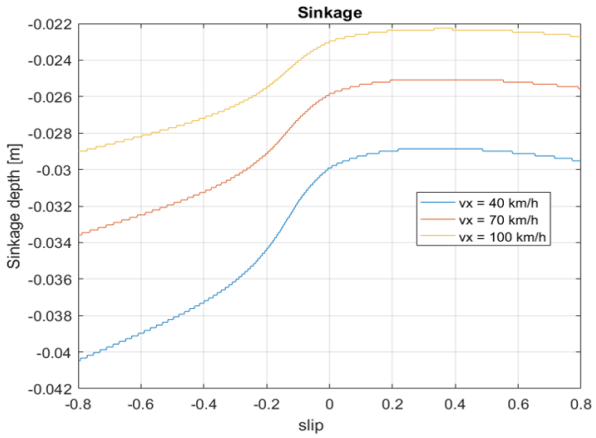

Figure 4.17: Sinkage depth with slip for different velocities. Here a large negative sinkage value indicates deep sinkage into the soil.

Longitudinal force

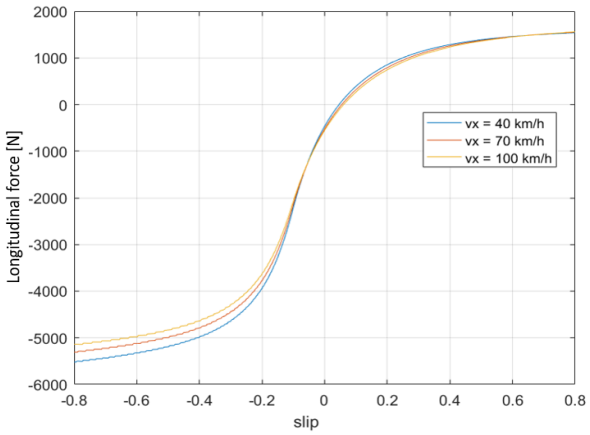

Figure 4.18: Longitudinal force with slip for different velocities.

From figure 4.17, we observe that sinkage depth for a given velocity say 40 km/h (blue line), decreases with increasing slip from -0.8 to 0. Sinkage depth reaches minimum around slip value of +0.3 and then increases again with slip. The decrease in sinkage height causes loss of contact angle which results in loss of traction force. The simulated curves for traction force for different velocities shown in 4.18 show that the traction force decreases in the regions where the sinkage height reduces.

Rolling Resistance

The rolling resistance decreases as expected of the model when the velocity is increased. The sinkage depth of the wheel reduces with increase in velocity which means there is lesser resistance to the tyre while rolling. This explains the lower values of rolling resistance force with increase in velocity.

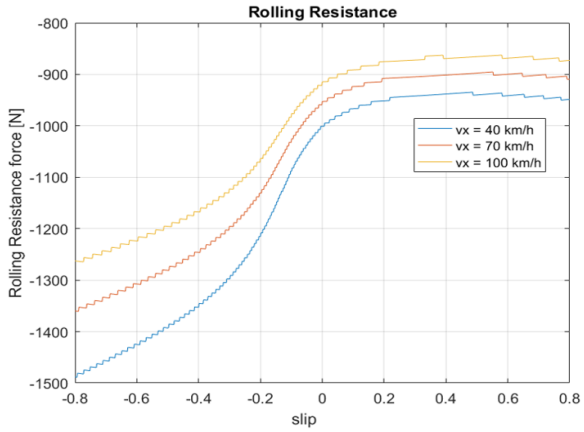

Figure 4.19: Rolling resistance with slip for different velocities

4.2.2.1 Validation

It is often very difficult to obtain measurement data for soft surface. Validation of the model is done by comparing simulation results with results from the paper [3], assuming same soil parameters.
The assumed soil parameters for this simulation are :

surface	k_1	k_2	n	c(Pa)	ϕ(deg)	$\gamma(N/m^3)$
sand	34	49.68	0.7	1150	31.1	15,696
moist loam	24.45	96.34	0.97	3300	33.7	15,196

Table 4.2: Soil property values used in the simulation for soft soil

The madel output:

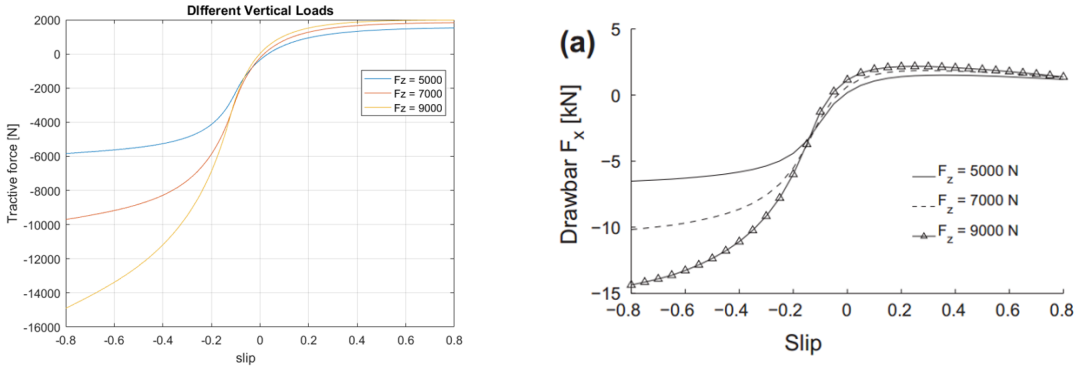

(a) **(b)**

Figure 4.20: (a): Model output (b): Simulation result from paper[3]

The two curves in the above figure exhibit similar trends. The model developed is successfully able to replicate the existing simulation output. The two curves saturate at similar levels braking force levels significantly higher than the driving force levels.

The influence of rolling resistance is very significant when it comes to soft surfaces. This large value gets added up on the braking side (both being negative) producing the resulting output curves.

5

Conclusions

5.1 Outcomes

Working models to calculate the rolling resistance and longitudinal force at the contact patch for hard surface and soft surface applications are built using Simulink and Matlab.

The results presented in this report were obtained by running just the tyre model independently. Although this tyre model can be integrated with the main energy model of AF consult.

Typical values of physical and emperical parameters for passenger cars is presented.

The results obtained from running the models is compared with available test data and/or model requirements for validation.

5.2 Hard Surface

The model simulations show that the improved brush model is capable of producing reliable results up to a slip range of about 30% and typical values of β for different surfaces are studied and tabulated. Since most car operations are within this slip limit it is reasonable to use the brush model up to these slip values.

The model gives closely matching results with experimental data even in the saturation region if the add-ons are active and some minimal parameters are tuned.

The impact loss approach for rolling resistance gives a physical explanation for the non-linear relationship of rolling resistance value with velocity.

The report also explains the non zero rolling resistance for zero velocity. The energy lost while the wheel is deformed and recovers its shape is due to mechanical energy dissipation in the form of heat and noise. This value depends on the extent of elasticity of the tyre.

5.3 Soft Surface

The developed model is consistent and gives physical explanations for the mechanics of soil-wheel interaction when a tire goes over a deformable surface. The simulated output results matches quite closely with the results published in paper[20].

Rolling resistance is a part of the model and included in the horizontal force equation. This eliminates the need to have a separate model for rolling resistance.

The influence of velocity on traction and sinkage depth is an addition to the model which predicts the desired trend satisfactorily.

There is a flexibility to select deformable tyre for the model which is empirical[9]. Validation of this concept is not a part of this thesis work and provided as a base for future work.

5.4 Future work

1. Temperature plays an important role in tyre performance because rubber material properties and inflation pressure differ with varying temperature. These temperature dependent effects can be added to both of the present models to improve the accuracy of results.
2. Tyre performance which includes tyre wear and loss due to vibration for different tyre patterns can be included to the models to make it more accurate.
3. The empirical parameters used in the add-ons can be generalized for different types of tyres and road surfaces by tuning the model with larder sets of test data when available.
4. The rolling resistance model for hard surfaces can be developed further by providing a physical explanation for the loss mechanism during flexing of tyres (sec 2.5.4). Finding test data of modern tyres to tune the values of ε_T and ε_F will be of significance for obtaining realistic results.
5. The flexible tyre model for soft surfaces can be developed by motivating the model with explanations based on physical principles.
6. The effect of sand/soil being thrown rearwards by a spinning wheel is not captured in the present model. This effect can be added to the current model to improve accuracy.
7. The computation time for running the soft soil model can be reduced by avoiding the iterations in the future.

Bibliography

[1] Bengt Jacobson, *Vehicle Dynamics Compendium*. Chalmers University of Technology, Sweden, 2016.

[2] Bekker, M. G. *Theory of land locomotion : the mechanics of vehicle mobility* . Ann Arbor : University of Michigan Press, [1962, 2d print.]

[3] C. Senatore, C. Sandu, *Journal of Terramechanics 48 (2011) 265–276*

[4] *Rhyne, T. B. "Development of a Vertical Stiffness Relationship for Belted Radial Tires," Tire Science and Technology, TSTCA, Vol. 33, no. 3, July-September 2005, pp. 136-155.*

[5] Jacob Svendenius, *Tire Modeling and Friction Estimation*, PhD thesis, 2007, Lund University

[6] Pope RG. The effect of wheel speed on rolling resistance, Journal of Terramechanics 1971;8(1):51–8

[7] I. Shmulevich a, U. Mussel, D. Wolf, The effect of velocity on rigid wheel performance, Journal of Terramechanics 35 (1998) 189–207

[8] John R.Smith and J.Charles Tracy, David S.Potter, Tire Rolling Resistance A Speed Dependent Contribution, SAE paper 780255 (1978)

[9] Brendan J. Chan, Development of an off-road capable tire model for vehicle dynamics simulations, PhD thesis, 2008, Virginia Polytechnic Institute

[10] Bharat Mohan, Redrouthu Sidharth Das, Tyre modelling for rolling resistance, Master's thesis 2014:24, Chalmers University of Technology

[11] Reece, A. R., 1964, "Problems of Soil-Vehicle Mechanics," Land Locomotion Laboratory (USATACOM), Warren, MI

[12] Karafiath, L. L., E. A. Nowatzki, 1978, Soil Mechanics for Off-Road Vehicle Engineering, Trans Tech Publications

[13] Wong JY, Reece AR. Prediction of rigid wheel performance based on analysis of soil–wheel stresses, part II. Performance of towed rigid wheels. J Terramechanics 1967;4(2):7–25.

[14] Shibly H, Iagnemma K, Dubowsky S. An equivalent soil mechanics formulation for rigid wheels in deformable terrain, with application to planetary exploration rovers. J Terramechanics 2005;42:1–13.

[15] Liang D, Hai-bo G, Zong D, Jian-guo T. Wheel slip-sinkage and its prediction model of lunar rover. J Cent South Univ Technol 2010;17:129–35.

[16] Michelin. 2001. The tyre Grip. u.o. : Michelin, 2001

[17] Gaetano Fortunato et. al, Dependency of Rubber Friction on Normal Force or Load: Theory and Experiment, Tire Science and Technology January-March 2017, Vol. 45, No. 1, pp. 25-54

[18] VTI data

[19] S.K. Clark, R.N. Dodge. A handbook for the rolling resistance of pneumatic tires, The university of Michigan, Ann Arbor 1979
[20] C. Senatore, C. Sandu. Off-road tire modeling and the multi-pass effect for vehicledynamics simulation, Virginia Tech, Blacksburg 2011
[21] Janosi Z, Hanamoto B. Analytical determination of drawbar pull as a function of slip for tracked vehicles in deformable soils. In: Proceedings of the 1st international conference on terrain-vehicle systems, Turin, Italy; 1961
[22] Zuzana Šabartová, A joint model of vehicle, tyres, and operation for the optimization of truck tyres, 4th International Tyre Colloquium 2015, pp. 177-186

A

Appendix 1

A.1 Flexible tyre Model

The model discussed in sec 4.2 assumes that the wheel is completely rigid. This means that the inflation pressure and the tyre material properties do not influence the output force on the contact patch. However, the wheel deforms to some extent along with the road surface. The tyre is divided into three parts with different radii and empirical relationships are defined to find each of these radii. The empirical relations also include some tyre construction properties. The equations are adopted from previous literature[9] and just presented in this thesis work as additional add-on. The model here has not been validated against any data and also not included in the main model itself.

As seen in fig A.1, a flexible ground and tyre combination leads to three different radii and hence leads to different load distributions.

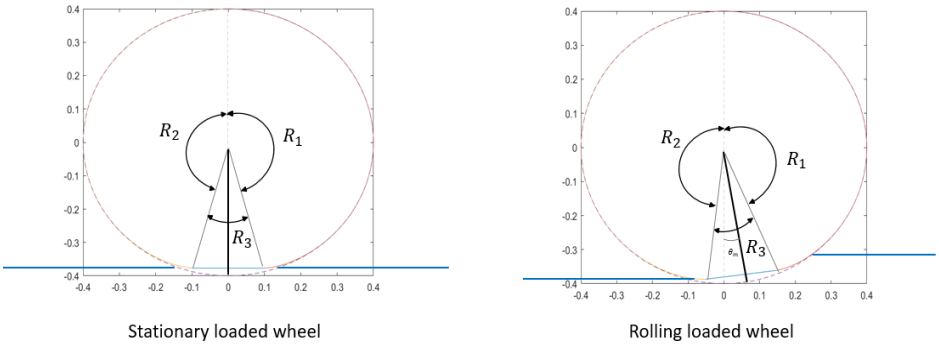

Figure A.1: Soil-wheel interaction for flexibly tyre

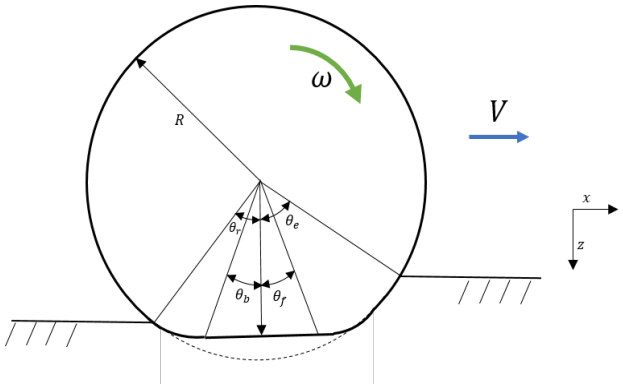

Figure A.2: Different angles formed during soil-wheel interaction on soft surface

The normal stress on the contact patch is given by the following equations :
for $\theta_e < \theta < \theta_f$,

$$\sigma_{f_1}(\theta) = (cK_1 + b\rho K_2)\left[R_2\left(\frac{\theta}{b}\right)(\cos\theta - \cos\theta_e)\right]^n \tag{A.1}$$

for $\theta_m < \theta < \theta_f$,

$$\sigma_{f2}(\theta) = (cK_1 + b\rho K_2)\left[R_1\left(\frac{\theta}{b}\right)(\cos\theta - \cos\theta_e)\right]^n \tag{A.2}$$

for $\theta_r < \theta < \theta_m$,

$$\sigma_{r1}(\theta) = (cK_1 + b\rho K_2)\left\{R_1\left(\frac{\theta}{b}\right)\left[\cos\left(\theta_e - \frac{(\theta - \theta_b)(\theta_e - \theta_m)}{\theta_m - \theta_b}\right) - \cos\theta_e\right]\right\}^n \tag{A.3}$$

for $\theta_b < \theta < \theta_r$,

$$\sigma_{r2}(\theta) = (cK_1 + b\rho K_2)\left\{R_3\left(\frac{\theta}{b}\right)\left[\cos\left(\theta_e - \frac{(\theta - \theta_b)(\theta_e - \theta_m)}{\theta_m - \theta_b}\right) - \cos\theta_e\right]\right\}^n \tag{A.4}$$

The verticals component of the normal stress is given by

$$\begin{aligned} F_{z\sigma} = {} & R_2 b \int_{\theta_e}^{\theta_f} \sigma_f \cos(\theta) d\theta + R_1 b \int_{\theta_f}^{\theta_m} \sigma_r \cos(\theta) d\theta \\ & + R_1 b \int_{\theta_m}^{\theta_r} \sigma_f \cos(\theta) d\theta + R_3 b \int_{\theta_r}^{\theta_b} \sigma_r \cos(\theta) d\theta \end{aligned} \tag{A.5}$$

Similarly, the expression for shear stress

$$\tau_{f1,2}(\theta) = \tau_{f_max}\Big(1 - e^{\frac{-J_{x1,2}}{k_x}}\Big) \tag{A.6}$$

$$\tau_{r3,4}(\theta) = \tau_{r_max}\Big(1 - e^{\frac{-J_{x3,4}}{k_x}}\Big) \tag{A.7}$$

where

$$\tau_{f1,2_{max}} = c + \sigma_{f1,2}(\theta)tan\phi \tag{A.8}$$

$$\tau_{f3,4_{max}} = c + \sigma_{f3,4}(\theta)tan\phi \tag{A.9}$$

$$J_{x_{1,2}} = R(\theta_{f1,2} - \theta - (1 - s_x)\sin\theta_{f1,2} - \sin\theta) \tag{A.10}$$

$$J_{x_{3,4}} = R(\theta_{f3,4} - \theta - (1 - s_x)\sin\theta_{f3,4} - \sin\theta) \tag{A.11}$$

A.2 User manual for simulink model

The model for computation of rolling resistance force and tractive force generated on the contact parch are combined into one Simulink module. A simplified view of the main blocks is shown in the figure A.3.
The developed tyre models are run independently (outside of the AF energy model). The input values are loaded as constant values for running the model. When integrated into the main energy model, some of these inputs become dynamic inputs coming in from the main vehicle model.

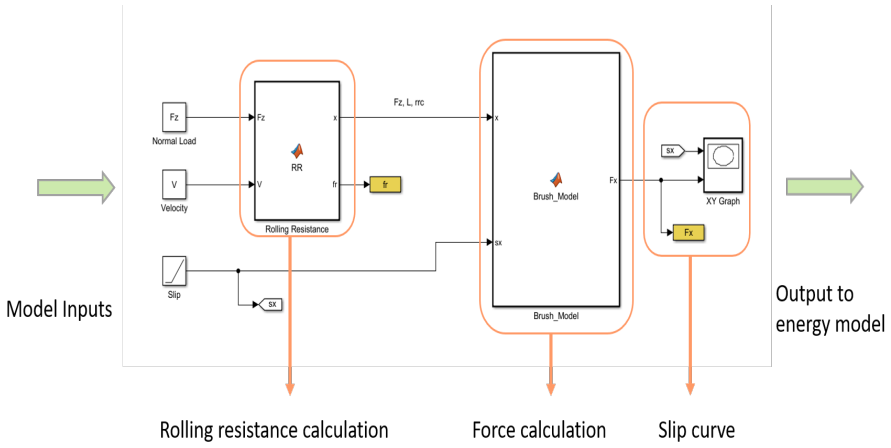

Figure A.3: Simulink model of hard surface

The model takes in inputs for normal load(Fz) and vehicle velocity(vx) in the form of constant blocks. Slip(sx) is given as a ramp input here ranging between -1 to +1. However, the model is flexible to take in dynamic inputs(for Fz,vx) from the main vehicle model while running a real simulation and calculate slip with the available wheel speed(ω) from the main vehicle model. Other parameters are scripted in a separate Matlab file called (initialize.m) that is executed at the beginning of every run. The model parameters are represented in the figure A.5.

The first function block contains equations to compute the contact patch length and rolling resistance force.
The contact patch length is then sent to the second block which contains the brush model equations to compute longitudinal force.
These values are plotted with normalized F_x $\left(\frac{F_x}{F_z}\right)$ on the x-axis and longitudinal slip (s_x) on the y-axis and saved in the workspace.

Note: It is not possible to use the SYMS command inside a function to perform integrations in the brush model equation. The integration was performed separately and the result was copied into the function block.

Sensitivity script
The sensitivity.m script contains plots for model sensitivity with different parameters. Depending on what parameter is studied, the user has to comment out the

relevant inputs in the initialize.m file so that the inputs are taken from the sensitivity.m file instead. The script has an execution command that will run the initialize.m file and the Simulink model file and produce the required plots. This holds good for the other sensitivity scripts as well

files associated with hard surface and rolling resistance

- Brushmodelnonsym.xls- main simulink model for hard surface and rolling resistance
- Initialize.m - initializes input parameters for both hard surface and rolling resistance
- sensitivity.m - to produce plots that check model sensitivity with various parameters for hard surface model
- RRsensitivity.m - to produce plots that check model sensitivity with various parameters for rolling resistance

Soft surface

The parameters are loaded into the model in the similar method discussed for hard surface. The main difference here is that the model has to be manually switched between rigid wheel (containing the Bekker-Reece equations) and flexible wheel discussed in section A.1 (containing empirical equations). The switch must be toggled at both 'variant source' and 'variant sink' for the model to work. The first block takes in the inputs and depending on the user's choice, the second block computes the longitudinal force on the contact patch and this is plotted as output and sent to the workspace.

As discussed before the sensitivity study script works exactly similar to the one for hard surface. The structure of the simulink model and associated parameters are shown below in figures A.4 and A.5 respectively.

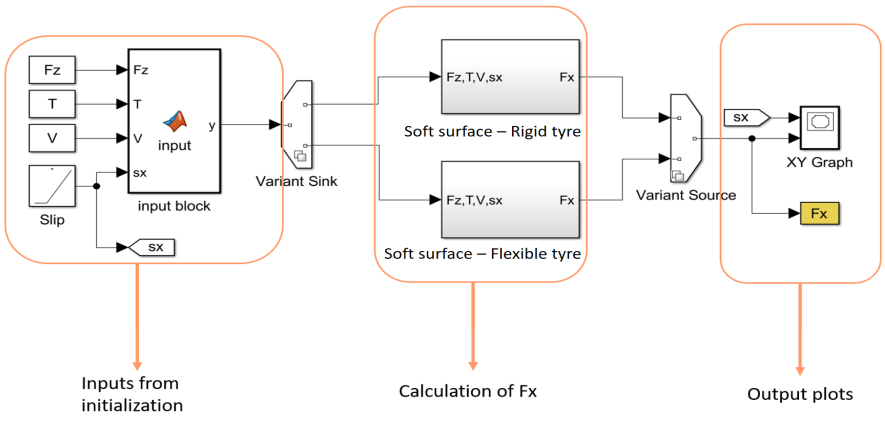

Figure A.4: Simulink model of soft surface with switch between rigid wheel and flexible wheel

The parameters required to run both the hard surface and soft surface models are shown in the figure below.

Hard surface parameters	Soft surface parameters	Common parameters for hard and soft surfaces
Radius (R)	Radius (R)	Radius (R)
Tyre Width (b)	Tyre Width (b)	Tyre Width (b)
Tread Height (H)	Inflation Pressure (P_i)	Inflation Pressure (P_i)
Inflation Pressure (P_i)	Coefficients to find value for θ_m	Sliding friction coefficient (μ_{slip})
Shear modulus of rubber (G)	Cohesion strength (c)	
Tuning factors for rolling resistance (ϵ_T, ϵ_F)	cohesive modulus of terrain deformation (k_1)	
Road friction coefficient for stick region (μ_{stick})	frictional modulus of terrain deformation (k_2)	
Road friction coefficient for slip region (μ_{slip})	sinkage exponent (n)	
Nominal tyre pressure (P_0)	Velocity dependence exponent (m)	
Nominal friction coefficient value (μ_0)	Sliding friction coefficient (μ_{slip})	
	Internal friction angle of the soil (ϕ)	
	Soil deformation module (k_x)	
	Soil density (ρ)	

Figure A.5: Parameters required for the models along with common parameters between the two models.

Note: all the files including the matlab scripts, simulink model and any associated measurement data should be in the same file directory for execution.

A.3 Matlab scripts

A.3.1 initialization - hard surface and rolling resistance

Some clean up

clc; clear all; close all;

Contents

%%%% Simulation parameters %%%%%%%%%%%%%%%%%%%%%%

```
sampleTime  = 0.01;             % Simulation Step Size [s]
simTime     = 10;               % Simulation end time [s]
```

Initialization Parameters

```
R = 0.611/2; % Radius of the tyre in m
W = 0.205; % width of tyre in m
P = 2.5; % Inflation pressure in bars or daN/cm^2
H = 0.01;%/(a4*(Fz/Fz0)+1-a4); % Tread height in m
%V = 13.88;
Fz = 5000;

a=1.5;
d = 200; % vertical damping stiffness of tyre
c = 200; % tyre vertical spring stiffness (no influence)
G = 1.1*8.63e04*a; % Longitudinal stiffness of the tyre
```

Road properties

```
 a1=1;
 a0=1;
mu_stk = a1; % friction co-efficient in stick region
mu_slp = a1/a0; % friction co-efficient in slip region
```

For mu varying with presure

```
P0 = 10e04;
mu0 = mu_stk/a0;
mu1 = 0.12;
```

Rolling Resistance

```
M =9.4; % kg
jt = 0.014 ; % factor for impact term
jf = 0.46; % factor for flexing term
```

A.3.2 Sensitivity - Hard surface

Contents

- Load sensitivity
- Diameter sensitivity
- Width Sensitivity
- Inflation pressure Sensitivity
- velocity influence
- Surface
- Inflation pressure Sensitivity

Load sensitivity

```
clear all
close all
R = 0.3;
W = 0.2;
P = 2.1;
V = 25;
omega = 60*5/18/R;
a1=1;       %[1:asphalt, 0.6:snow, 0.08:Ice]
a0=1.42;    %[1.42:asphalt, 1:snow, 1:Ice]

% case 1
Fz=6000;
sim('Brush_Model_nonsym')
figure(1)
plot(sx,Fx)
grid on
hold on

%case 2
Fz=4000;
sim('Brush_Model_nonsym')
plot(sx,Fx)
xlabel('slip ratio') % x-axis label
ylabel('Longitudinal Force [N]') % y-axis label
legend('Fz=6000 N','Fz=4000 N')
title('Load Sensitive study')
```

Diameter sensitivity

```
% case 1
R = 0.4;
sim('Brush_Model_nonsym')
figure(2)
plot(sx,Fx)
grid on
hold on

%case 2
R=0.3;
sim('Brush_Model_nonsym')
plot(sx,Fx)
xlabel('slip ratio') % x-axis label
ylabel('Longitudinal Force[N]') % y-axis label
legend('R=0.4 m','R=0.3 m')
title('Diameter senstive study')
```

Width Sensitivity

```
% case 1
W = 0.25;
sim('Brush_Model_nonsym')
figure(3)
plot(sx,Fx)
grid on
hold on

%case 2
W=0.2;
sim('Brush_Model_nonsym')
plot(sx,Fx)
xlabel('slip ratio') % x-axis label
ylabel('Longitudinal Force [N]') % y-axis label
legend('W=0.25 m','W=0.2 m')
title('Width sensitive study')
```

Inflation pressure Sensitivity

```
% case 1
P = 1.5;
sim('Brush_Model_nonsym')
figure(4)
plot(sx,Fx,'b',sx,rrc.*Fz,'-.b')
grid on
hold on
```

```
%case 2
P =2.5;
sim('Brush_Model_nonsym')
plot(sx,Fx,'r',sx,rrc.*Fz,'-.r')
xlabel('slip ratio') % x-axis label
ylabel('Longitudinal Force [N]') % y-axis label
legend('P1 = 1.5 bar','rolling resistance at P1','P2 = 2.5 bar','rolling resistance
title('Inflation pressure sensitive study')
```

velocity influence

```
% case 1
omega = 10*5/18/R;
sim('Brush_Model_nonsym')
figure(5)
plot(sx,rrc*100)
grid on
hold on

%case 2
omega = 100*5/18/R;
sim('Brush_Model_nonsym')
plot(sx,rrc*100)
xlabel('slip ratio') % x-axis label
ylabel('rolling resistance: rrc*100') % y-axis label
legend('Vx = 10 kmph','Vx = 100 kmph')
title('Velocity sensitive study')
```

Surface

```
a1=1;
a0 = 1.42;
omega = 60*5/18/R;

sim('Brush_Model_nonsym')
figure(6)
plot(sx,Fx)
grid on
hold on

a1 = 0.4;
a0 = 1;
sim('Brush_Model_nonsym')
plot(sx,Fx)
hold on
```

```
a1 = 0.08;
a0 = 1;
sim('Brush_Model_nonsym')
plot(sx,Fx)
hold off

xlabel('slip ratio') % x-axis label
ylabel('Longitudinal Force [N]') % y-axis label
legend('Asphalt, mu = 1','Snow, mu = 0.4','Ice, mu = 0.08')
title('Different Surfaces')
```

Inflation pressure Sensitivity

```
% case 1
P1 = [0.5 1 1.5 2 2.5 3 3.5 4];
for i = 1:length(P1)
Pi = P1(i);
sim('Brush_Model_nonsym')
figure(7)
plot(Pi,rrc.*100,'*')
grid on
hold on
end
hold off

xlabel('Tyre pressure [bar]') % x-axis label
ylabel('rolling resistance: rrc*100') % y-axis label
%legend('P=1.5 bar','P = 2.5 bar')
title('Inflation pressure sensitive study')
```

A.3.3 Rolling resistance model

```
%close all
%clear all

 V=(5/18)*linspace(0,180,1000); %vehicle velocity in meters per second

 v=V*18/5; %kmph
%V=16.7;%vehicle velocity in meters per second
run 'InitializeModel'
%Fz = 5000;
Kz = 0.0274*P*((W*2*R*10^6)^0.5) + 3.38; % in daN/mm
Re = R -(Fz/Kz/10^4); % in m
kmax = acos(Re/R);% in rad
L = 2*(R^2 - Re^2)^0.5;
```

```
%del=R-Re;
alpha = asin(L/(2*R));
p_g  = Fz/(W*L);

for i=1:length(V)

T(i)    = ((M.*V(i).^2)/(2*pi))*(1-cos(alpha));
P_t(i)  = V(i).*T(i)/Re;
U_t(i)  = P_t(i)*jt;
A_f(i)  = (2*pi*p_g.*W)*((pi*R^2*(alpha/pi))-(Re)*(L/2))/(alpha*2);
p_f(i)  = A_f(i).*V(i)/(pi*2*R);
U_f(i)  = p_f(i)*(jf);

rt(i)   = U_t(i)./V(i)/Fz;
rf(i)   = U_f(i)./V(i)/Fz;
rrc(i)  = (rt(i)+rf(i));
end

figure(1)

plot(v,rrc*(50),'r')
xlim([0,200]);
ylim([0,2]);
xlabel('velocity (kmph)');
ylabel('Fx/Fz (daN/1000)');
%title('Simulation plot - velocity vs normalized Fx');
hold on

%loading test data
% load 'rr_expt_data'
% plot(x_009,y_009/10,'b')
% legend('simulation result','test data','location','Northeast')
% %t = annotation('textbox');
% %sz = t.FontSize;
% %t.FontSize = 12;
% grid minor
% hold on
```

A.3.4 Sensitivity - rolling resistance

Contents

- Diameter sensitivity
- Width Sensitivity
- Load Sensitivity
- saving files

```
%RR sensitivity
clear all
```

```
clc
close all

R = 0.622/2; % Radius of the tyre in m
W = 0.185; % width of tyre in m
P = 2.5; % Inflation pressure in bars or daN/cm^2
H = 0.01;%/(a4*(Fz/Fz0)+1-a4); % Tread height in m
M=8;
Fz=5000;

figure(1)
% load 'rr_expt_data'
% plot(x_006,y_006/10,'b')
% legend('simulation result','test data','location','Northeast')

grid minor
hold on
%%mass sensitivity
%case 1
M=6;
run 'RR'

plot(v,rrc*(50),'r')
xlim([0,200]);
ylim([0,2]);
xlabel('velocity (kmph)');
ylabel('Fx/Fz (daN/1000)');
hold on

%case 2
M=8;
run 'RR'

plot(v,rrc*(50),'b')
xlim([0,200]);
ylim([0,2]);
xlabel('velocity (kmph)');
ylabel('Fx/Fz (daN/1000)');
hold on

%case 3
M=10;
run 'RR'

plot(v,rrc*(50),'g')
xlim([0,200]);
```

```
ylim([0,2]);
xlabel('velocity (kmph)');
ylabel('Fx/Fz (daN/1000)');
title('Tyre Mass sensitivity');
legend('M=6 Kg','M=8 Kg','M=10 Kg','location','Northeast')
hold off
```

Diameter sensitivity

```
figure(2)
%case 1
R=0.500/2;
run 'RR'

plot(v,rrc*(50),'r')
xlim([0,200]);
ylim([0,2]);
xlabel('velocity (kmph)');
ylabel('Fx/Fz (daN/1000)');
hold on

%case 2
R=0.622/2;
run 'RR'

plot(v,rrc*(50),'b')
xlim([0,200]);
ylim([0,2]);
xlabel('velocity (kmph)');
ylabel('Fx/Fz (daN/1000)');
hold on

%case 3
R=0.800/2;
run 'RR'

plot(v,rrc*(50),'g')
xlim([0,200]);
ylim([0,2]);
xlabel('velocity (kmph)');
ylabel('Fx/Fz (daN/1000)');
title('Diameter sensitivity');
legend('D=0.5 m','D=0.62 m','D=0.8 m','location','Northeast')
grid minor
hold off
```

Width Sensitivity

```
figure(3)
%case 1
W=0.15;
run 'RR'

plot(v,rrc*(50),'r')
xlim([0,200]);
ylim([0,2]);
xlabel('velocity (kmph)');
ylabel('Fx/Fz (daN/1000)');
hold on

%case 2
W=0.185;
run 'RR'

plot(v,rrc*(50),'b')
xlim([0,200]);
ylim([0,2]);
xlabel('velocity (kmph)');
ylabel('Fx/Fz (daN/1000)');
hold on

%case 3
W=0.22;
run 'RR'

plot(v,rrc*(50),'g')
xlim([0,200]);
ylim([0,2]);
xlabel('velocity (kmph)');
ylabel('Fx/Fz (daN/1000)');
title('Width sensitivity');
legend('W=0.15 m','W=0.185 m','W=0.22 m','location','Northeast')
grid minor
hold off
```

Load Sensitivity

```
figure(4)
%case 1
Fz=3000;
run 'RR'

plot(v,rrc*(50),'r')
```

```
xlim([0,200]);
ylim([0,2]);
xlabel('velocity (kmph)');
ylabel('Fx/Fz (daN/1000)');
hold on

%case 2
Fz=5000;
run 'RR'

plot(v,rrc*(50),'b')
xlim([0,200]);
ylim([0,2]);
xlabel('velocity (kmph)');
ylabel('Fx/Fz (daN/1000)');
hold on

%case 3
Fz=7000;
run 'RR'

plot(v,rrc*(50),'g')
xlim([0,200]);
ylim([0,2]);
xlabel('velocity (kmph)');
ylabel('Fx/Fz (daN/1000)');
title('Normal Load sensitivity');
legend('Load=3000 N','Load=5000 N','Load=7000 N','location','Northeast')
grid minor
hold off
```

A.3.5 Initialization - soft soil

```
# Some clean up

clc; clear all; close all;


## Contents

- %%%% Simulation parameters %%%%%%%%%%%%%%%%%%%%%%
- Model Selection
- Initialization Parameters
- Flexible tyre
```

%%%% Simulation parameters %%%%%%%%%%%%%%%%%%%%

```
sampleTime  = 0.01;            % Simulation Step Size [s]
simTime     = 10;              % Simulation end time [s]
```

Initialization Parameters

```
% Vehicle properties
% Tyre properties // Continental Contitrac SUV P265/70/R17
r  = 0.4;
b  = 0.265;
c0 = 0.4;
c1 = 0.2;
g  =-0.0;

% Dry Sand
c = 1150;                  % [Pa] cohesion strength
k1 = 34;                % kc,coeffieint in bekker pressure sinkage expression
k2 = 49.68;             % kp,coeffieint in bekker pressure sinkage expression
n = 0.3;%0.7;                  % sinkage exponent
v0 = 60*5/18;
v1 = 2;
m = 1;%0.3 or 1;                   % velocity dependence exponent
mu = 0.7;                 % sliding friction coefficient of Dry sand
phi = 31.1*pi/180;        %[radians], angle of internal friction of the soil
kx = 0.015;               % soil deformation module for zero side slip angle
rho = 15696;               %[N/m3] density of soil*g

% % Moist loam
% c = 22670;                  % [Pa] cohesion strength
% k1 = 3.25;                % kc,coeffieint in bekker pressure sinkage expression
% k2 = 4600;             % kp,coeffieint in bekker pressure sinkage expression
% n = 0.99;                 % sinkage exponent
% v0 = 60*5/18;
% v1 = 2;
% m = 1;%0.3 or 1;                   % velocity dependence exponent
% mu = 0.4;                 % sliding friction coefficient of Dry sand
% phi = 22*pi/180;        %[radians], angle of internal friction of the soil
% kx = 0.015;               % soil deformation module for zero side slip angle
% rho = 1258*9.8;               %[N/m3] density of soil*g
```

Flexible tyre

```
d0 = 0.0230;              % delta, deflection in the tire [m]
z0 = 0.0845;              % zeta
b0 = 6.3579;              % beta
```

A.3.6 sensitivity - soft soil

Velocity sensitivity

```
clear all
close all

vx = 20*5/18; % 20 km/h
% case 1
% Rigid wheel or flexible tyre model
m0 = 1; %[1,2]=[rigid,flexible] tyre model
M0 = Simulink.Parameter(m0);
sim('Sand_Model')
figure(1)
plot(sx,Fx,'b')
grid on;hold on
figure(2)
plot(sx,s0,'b')
grid on;hold on
% case 2
m0 = 2; %[1,2]=[rigid,flexible] tyre model
M0 = Simulink.Parameter(m0);
sim('Sand_Model')
figure(1)
plot(sx,Fx,'r')
figure(2)
plot(sx,s0,'r')
legend('Rigid','Flexible')

clear all
close all

m0 = 1; %[1,2]=[rigid,flexible] tyre model
M0 = Simulink.Parameter(m0);
%case 2
vx = 40*5/18; % 100 km/h
sim('Sand_Model')
figure(3)
plot(sx,Fx)
grid on
hold on
figure(4)
plot(sx,s0)
grid on
hold on
```

```
%case 3
vx = 70*5/18; % 100 km/h
sim('Sand_Model')
figure(3)
plot(sx,Fx)
figure(4)
plot(sx,s0)


%case 4
vx = 100*5/18; % 100 km/h
sim('Sand_Model')
figure(3)
plot(sx,Fx)
figure(4)
plot(sx,s0)

% xlabel('slip ratio') % x-axis label
% ylabel('Longitudinal Force [N]') % y-axis label
% legend('vx = 10 km/h','vx = 40 km/h','vx = 70 km/h','vx = 100 km/h')
% title('Velocity Sensitive study')
```